UNIVERSIDADE NOVA DE LISBOA

Faculdade de Ciências e Tecnologia

Departamento de Engenharia Mecânica e Industrial/Secção de Tecnologia Industrial

Modelling a Cable Structure for a New Wind Energy Production Device

Por

Miguel Pita Soares da Fonseca Calvário

Dissertação apresentada na Faculdade de Ciências e Tecnologia da Universidade Nova de Lisboa para obtenção do grau de Mestre em Engenharia Mecânica Especialização em Concepção e Produção

2ºCiclo

Orientador: Prof. Jorge Joaquim Pamies Teixeira

Co-orientador: Eng.º Tiago Pardal

Lisboa

2010

Acknowledgements

Writing this thesis was only possible due the collaboration of several persons, to which I want to express my thanks, especially:

- To my supervisor, Prof. Jorge Joaquim Pamies Teixeira, I thank the opportunity to develop this thesis and for the different meetings, suggestions and guidance (have in mind his long experience) during the supervising process;
- To OMNIDEA, for the challenge of participating on this innovative project. I'm particulate grateful to my co-supervisor, Eng.º Tiago Pardal, for availability of commercial information, to Eng.º Pedro Silva for his opinions and special support on the computational domain and to Eng.º Nuno Fernandes for his suggestions to the structure of thesis.
- To Prof. João Burguete Cardoso for the support given on the modulation and analysis of the cable structure;
- To teachers and partners of Faculdade de Ciências e Tecnologia of Universidade Nova de Lisboa and Escola Superior de Tecnologia of Instituto Politécnico de Setúbal that contributed to my engineering formation.

Abstract

The following thesis subject is based on the identification and dimensioning of the main mechanical components of the ground station of Boreas prototype, as well as a three-dimensional finite element analysis of structural cable that connects the ground station to the module's air system. The module powered by a lift force pulls a cable that drives a mechanical system which in turn drives a generator during the productive phase of the energy cycle. In the other phase, the system inverts the turn and energy is consumed. The production of energy should be greater than the energy consume.

The dimensioning of main mechanical components of ground station includes: flywheel, cable, capstan drum and winder drum.

Structural analysis of the cable is performed with an algorithm based on a three-dimensional finite element analysis, which allows the control of cable tension on the end of capstan, prevent the rupture of cable, avoid high forces on bearings and the shock between the rope and the ground. The results of programme developed with the algorithm, are compared with the results obtained by an analytical approach and with commercial software of finite elements.

This thesis contributes to the realization of mechanical components included in the prototype.

Keywords: mechanical system, cable, modulation of finite elements

Resumo

A presente tese tem como objectivos a identificação e dimensionamento dos principais componentes mecânicos da estação terrestre do protótipo Boreas, bem como uma análise tridimensional de elementos finitos do cabo estrutural que une a estação terrestre ao módulo aéreo do protótipo. O módulo aéreo movido por uma força de sustentação aerodinâmica puxa um cabo que acciona um sistema mecânico que por sua vez conduz um gerador durante a fase produtiva do ciclo energético. Na outra fase do ciclo, o sistema inverte o sentido do movimento, consumindo energia. A produção energética deverá superar o consumo energético.

O dimensionamento dos principais componentes mecânicos da estação terrestre inclui: volante, cabo, tambores do cabrestante e enrolador.

A análise estrutural do cabo é desenvolvida através de um algoritmo baseado numa análise de tridimensional de elementos finitos, permitindo o controlo da tensão de cabo no apoio situado no cabrestante, previne a ruptura do cabo, evita forças elevadas nos rolamentos e o choque entre o cabo e o chão. Os resultados do programa desenvolvido com o algoritmo são comparados com os resultados obtidos por um método analítico e por um software comercial de elementos finitos.

Esta tese contribui para a materialização dos componentes mecânicos incluídos no protótipo.

Palavras-chave: sistema mecânico, cabo, modulação por elementos finitos

Nomenclature

c_1 c_2	Constants of integration
D_{ec}	Diameter of electric cable
D_{ext}	External diameter of the ring
D_{extg}	External diameter of gas tube
D_{flange}	Diameter of flange
D_{int}	Inner diameter of the ring
D_{intg}	Internal diameter of gas tube
E_{UHMPE}	Young modules of UHMPE
E_{steel}	Young modules of steel
F_{winder}	Force on winder drum
$F_{Unwinding}$	Force of unwinding
$F_{capstan}$	Force on capstan drum
F_{drag}	Drag force
F_{max}	Maximum force of operation
F_{min}	Minimum force of operation
G_i	Weight of their own half of the distributed force
L_{t}	Total length of cable
L_{winder}	Length of winder
R_a	Results from programmes or analytical solution
R_s	Results from software
T_0	Axial force on the vertex of catenary
V_{ec}	Unitary Volume of electric cable
V_{gt}	Unitary Volume of gas tube
W_{cable}	Total weight of cable
$W_{catcable}$	Weight of catenary cable for unit of length
W_{ec}	Weight of the electric cable for unit of length
$W_{element}$	Weight of elements
W_{gt}	Weight of gas tube for unit of length
W_{sc}	Weight of structural cable for unit of length
d_i	Vector of total displacements (iteration i)

d_{i+1}	Vector of total displacements (iteration i+1)
$f_1, f_2, f_3, f_4, f_5, f_6$	Internal forces
f_{ext}	External forces vector
f_{int}	Internal forces vector
l_0	Initial length (m)
l_1	Length of cable
l_2	Length of catenary
l_3	Length of parabola
l_i	Length of cable for a certain loop
l_x, l_y, l_z	Projection of element l in the three orthogonal axes
$n_{elements}$	Number of elements
$p_{capstan}$	Pressure on capstan drum
p_{winder}	Pressure on winder drum
r_1	Inner radius of capstan drum
r_2	Outer radius of capstan drum
r_{Shaft}	Radius of shaft
r_{cable}	Radius of cable
$r_{capstan}$	External Radius of capstan drum
$r_{capstani}$	Inner Radius of capstan drum
r_i	Radius of the pack (winder drum+ loops of cable)
r_{winder}	Radius of winder drum
$r_{winderext}$	External radius of winder drum
$r_{winderint}$	Internal radius of winder drum
$r_{windermed}$	Variable radius between $r_{winderint}$ an $r_{winderext}$
$t_{hflywheel}$	Thickness of flywheel
$t_{hcapstan}$	Thickness of capstan drum
$t_{hwinder}$	Thickness of winder drum
$x_0, y_0, z_0, x_1, y_1, z_1$	Nodal coordinates
ε_r	Radial strain
ε_t	Tangential strain
$\rho_{polyamide}$	Density of polyamide
ρ_{copper}	Density of cooper

ρ_{steel}	Density of steel
$\sigma_1, \sigma_2, \sigma_3$	Principal stresses
$\sigma_{Service}$	Stress of service
$\sigma_{Ultimate1}$	Ultimate stress on cable
$\sigma_{Ultimate2}$	Ultimate stress on capstan drum
$\sigma_{allowable1}$	Maximum allowable stress on cable
$\sigma_{allowable2}$	Maximum allowable stress on capstan drum
σ_{max}	Maximum stress on cable
σ_r	Radial stress
σ_θ	Tangential stress
$\sigma_{\theta 1}$	Tangential stress due external pressure on winder drum
$\sigma_{\theta 2}$	Tangential stress due the rotation of winder drum
ω_{motor}	Angular speed of motor
Δd_i	Incremental displacement vector
FEM	Finite element method
UHMPE	Ultra high molecular polyethylene
D	Diameter of capstan drum
E	Young modules
En_l	Energy lost
En_s	Energy stored
En_{se}	Energy stored effectively
En	Energy
$Error$	Approximation error
I	Inertia moment of flywheel
K	Tangent stiffness matrix
MBF	Minimum breaking force
P	Power
R	Relation of the load side and hold side
Re_{max}	Maximum relative error
Re_{min}	Minimum relative error
Re	Relative error
S	Relation between L_{winder} and d
Sf_1	Safety factor for cable

Sf_2	Safety factor for capstan drum
T	Axial force on a point
c	Constant parameter of the curve
d	Diameter of structural cable
g	Acceleration of gravity
i	Number of turns in section
k	Sub-matrix
l	Deformed length
r	Inner radius of cylinder
$s(r_{windermed})$	Tensile stress
t	Time
u	Displacement of the cylindrical surface of radius r
v	Speed
x	Abscissa of a point
y	Ordinate of a point
Ω	Area of cross section
γ	Friction coefficient
ε	Lagrange-Green strain
μ	Poisson ratio
$\sigma(\varepsilon)$	Uniform stress on the element
ω	Angular speed of capstan
$r_{cylinder2}$	Cylinder external radius of
$r_{cylinder1}$	Cylinder inner radius of

General index

Figures index

Tables index

1. Introduction

The tendencies for future solutions of wind energy production, in opposition to actual wind systems (for example wind turbines), are constituted by aero structures, lighter than air. In this way the system, which is described, is an aero structure that work in cycles of high altitudes (more than 500 meters) being connected to a capstan on the ground. This system is coupled to an electric generator, producing energy during a part of cycle. The system is currently patented, [**1**].

The importance of working with the wind of high altitudes is reflected on the electric power. The value of wind speed increases with the increasing of altitude and the electrical power generated by wind turbines in the process of energy transformation shows a cubic dependence on wind speed, so small variations in wind speed represent large variations on value of electric power, [**2**]. The wind speed at 450 meters can be four or five times higher than in the ground, [**2**], and its flow is more stable than the earth surface reducing the problem of seasonality.

The objectives of this thesis are the identification and dimensioning of the main mechanical components of the ground station (flywheel, cable, capstan drum and winder drum) of Boreas prototype as well as a three-dimensional finite element analysis of structural cable that connects the ground station to the module's air system. Under the scientific point of view, the modelling of cable structure is studied to allow the determination of stresses and cable trajectory. The importance of knowing which is the tension on the rope for the different nodes and the angle between cable and ends is to prevent the rupture of cable, avoid high forces on bearings and avoid the shock between the rope and the ground (which creates too friction on cable). The displacements (due the elasticity of cable and value of loads) are an important issue taking into account the limited area of work.

On the future work other components as the support structure of the drum, the structure of anchoring to the ground, the control system, etc, should be studied in order to complete the design of prototype.

2. Thesis structure

The thesis is structured in 7 chapters. Chapter 1 consists on an introduction to the general environment of wind energies where considerations about the importance of wind of high altitudes are mentioned. The chapter continues with a short description of the mechanical system and the future work. Chapter 3 presents a state of art of wind technologies where the characteristics of wind resource and the technologies that take part of it are in discussion.

Chapter 4 refers to a description of the characteristics of the "Boreas" prototype, where the elements of the mechanical device are mentioned.

The chapter 5 is related to the energy considerations and with the dimensioning of major mechanical components of ground station (flywheel, cable, capstan drum, winder, respectively). In this way data is provide for the design of prototype.

On chapter 6, the methodology and proposed modelling of cable structure is presented considering two possible approaches based on analytical equations or the finite element method. Later in the chapter an algorithm characterizing the behaviour of cable submitted to forces is proposed. This algorithm will be important for the control programme of the device.

On chapter 7 the thesis conclusion is presented and the future work to be done is proposed. Lastly, the thesis has 5 annexes being the first one related to the list of MATLAB file, the Annex 2 and 3 represent the input files of programme's A and programme's version B, the Annex 4 specifies the ANSYS file and on Annex 5 is shown the input file of the structural analysis of cable example.

3. State of art of wind technologies

This topic, after an introduction to the thematic of wind resource, describes the major technologies that take part from the wind resource in order to produce energy; in particular electric energy.

3.1. The wind resource

The wind can be characterized as air in motion with a certain intensity and direction. It is the result from displacement of air masses, as a result of pressure differences between two distinct regions. The pressure differences are associated with solar radiation and heating processes of air masses: the high pressure air descends and departs heating to converge and where the low rises, [**2**]. The heating areas of land and sea are different from the poles to the tropics, causing the displacement of heat flows between these zones, being the wind one of carriers of heat flows. The wind would always flow perpendicular to the isobars if the influence of rotation of the earth does not induced small deviations in the flow of wind through the action of Coriolis forces, [**2**].

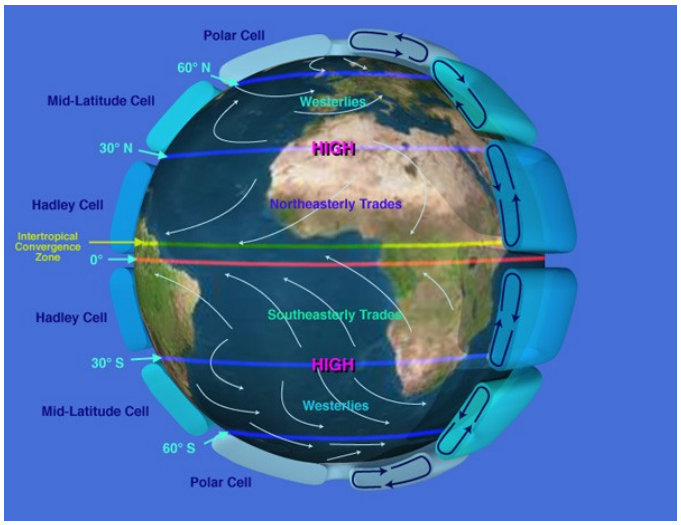

Figure 3.1 - Earth circulation cells, [3].

Other important issue are the breezes, which refers to the flow localized wind with lower intensity. The breezes result from the unequal heating or cooling of land surfaces, on a certain location. The most common breezes are, [**2**]:

- Land breeze - Wind that blows during the night of earth surface into the sea, in that, on the earth surface the temperature decreases more quickly in the night, compared with sea water, creating a difference of pressure; high pressures on the earth surface and low pressures on the sea;
- Sea breeze - Wind that blows during the day, from the sea to earth surface and as result of the earth surface warm more quickly than sea water during the day, a difference of pressure is created; high pressures on the sea and low pressures on the earth;
- Valley breeze - Winds that blows in the morning from the valley to the mountains peaks and, as a result of the mountains peaks warm faster than the valleys, a difference of pressure is creating; high pressures on the valley and low pressures on the mountain peaks.

The increase of altitude increase the wind speed, due the roughness, orography but also because the air is denser on the earth surface, decreasing the density with height, [**2**]. The wind speed don't increases infinitely with the increase of height from the ground, it can be to 450 meters four or five times higher than in the ground but at higher levels the relation decreases, [**2**].

The knowledge of the wind behaviour is determinate to introduce the technology on a certain place in order to adjust parameters, as the height or orientation of structure.

3.2. Wind technologies

The wind technologies are one type of the renewable energies and are characterized specially by the wind turbines.

3.2.1. Reference to wind turbines

The wind energy can be described as the transformation of energy provided by wind on a useful energy, generally electricity. The most known way to produce wind energy is the use of wind turbines, which drive an electric generator.

The main components that constituted the wind turbines are:

- Blade – Component that is orientated to wind direction in order to rotate;
- Hub – Joint of blades with the shaft, which will transmit horse power;
- Nacelle – Component that includes: the anemometer, bearings, rotor, gearbox, generator, coupling, disk brake yaw system, etc.
- Tower – Element that brings height to structure;
- Foundation – Element that holds the tower and others components to ground.

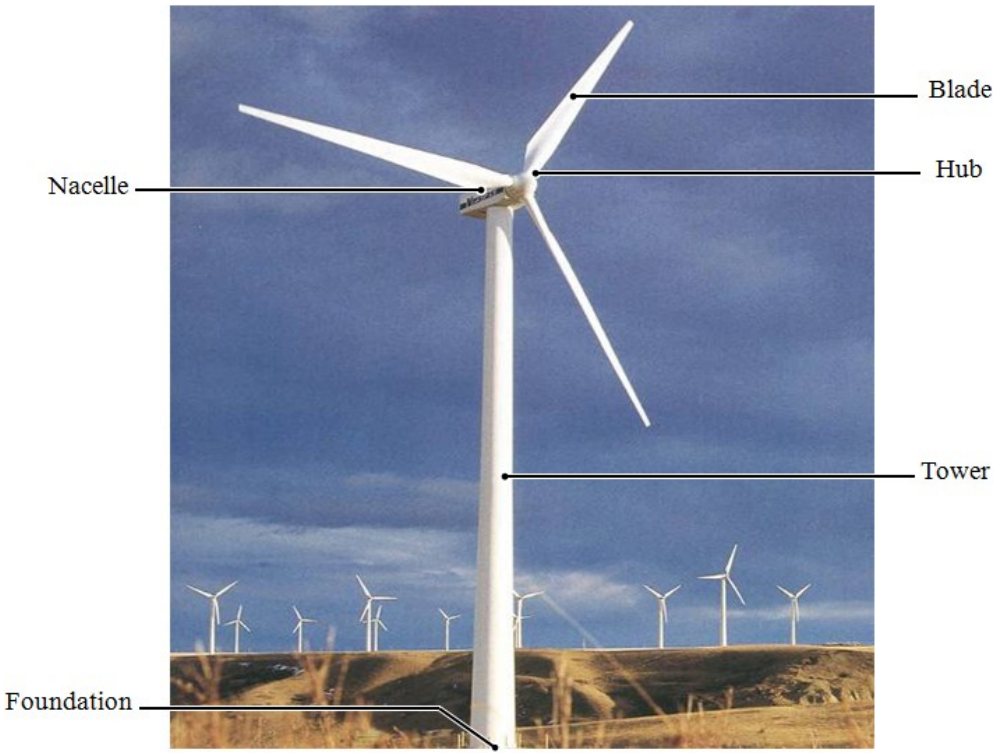

Figure 3.2 - Main parts of a wind turbine. Adapted from [4].

The principle that allows the transformation of wind energy in electric energy is described as a result of using the aerodynamic principles; in particular two primary aerodynamic forces: lift force, in the direction perpendicular to wind flow, and drag force in direction parallel to wind flow. The turbine blades use an airfoil design, in which one surface is nearly rounded and the other is relatively flat. When the wind flows into the rounded surface, the air is forced to rise, increasing velocity. The faster moving air tends to rise in the atmosphere due to a decrease in pressure just above of the curved surface. On the upwind side of the blade, the wind is moving slower,creating an area of higher pressure that pushes on the blade, trying to slow it down. This difference in pressure implies that the low-pressure area sucks the blade towards the wind flow, creating the lift force that is perpendicular to drag force, [**5**].

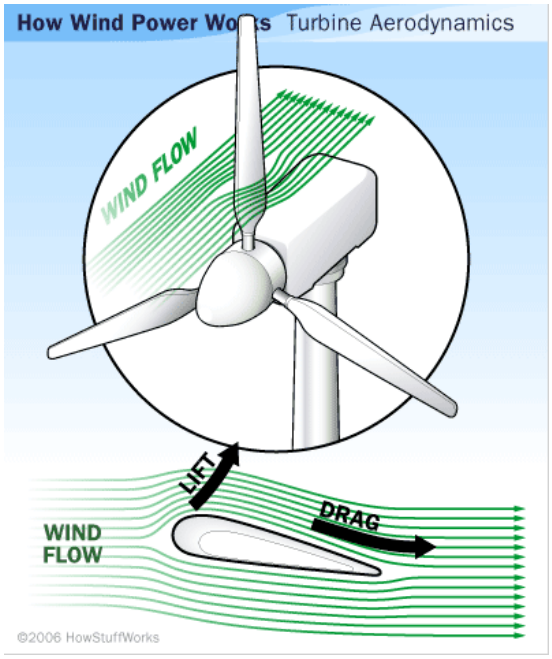

Figure 3.3 - Illustration of the principle of operation of wind turbines, [5].

The aerodynamic principles are not the only parameters on the design of wind turbines. For example the size of blade is quite important because the longer be the turbine blades are, greater is the diameter of the rotor and more energy can be produced. As a rule, doubling the rotor diameter produces a four times more energy. However it must to be taken into account that the increase of inertia on the system requires more power to spin the generator and therefore a trade should be obtained between these aspects.

The tower height is also an important parameter in production capacity, heaving in mind that higher elevations allow higher wind speed because, at the ground friction and heights of

objects interrupt the wind of flow, reducing the wind speed, [**5**]. In this way higher turbines can capture more energy.

In order to calculate the power of the wind turbine is important to know the wind velocity at the place of implementation and nominal capacity of wind turbine (dimensions, rotor diameter and other). The major part of turbines reach their maximum power at speeds of wind near 15 (m/s), and if be considerate stable winds the rotor diameter determinates the quantity of energy to produce. At the time that rotor diameter increases, the height of the tower increase as well, which allows to access to faster winds, [**5**].

It is important to note that at 15 (m/s) the generality of turbines reach his nominal capacity and at 20 (m/s) the system is shut down, [**5**], because at that wind speeds the structure can collapse specially due the large vibrations.

At a global scale, the installed capacity by the end of 2009 reached 158.505 (MW) and 38.343 (MW) were added, [**6**]. The average capacity of wind turbines installed globally in 2007 was 1492 (kW), [**7**] , and the largest turbines on the market have now 6 (MW) in capacity, [**8**].

3.2.2. Mention to MARS project

At the moment, a new dispositive called MARS (Magenn Power Air Rotor System) is being developed and it consists on a rotor device, lighter than air that rotates about a horizontal axis due the wind and his rotation is converted into electrical energy. The electrical energy is transported down to a transformer at a ground station; being transported to the electricity power grid. The air rotor is sustained by helium and the rotor lights to the more adequate altitudes taking in account the wind speed, which also causes the Magnus effect creating additional lift which keeps the device stabilized and positioned, [**9**].

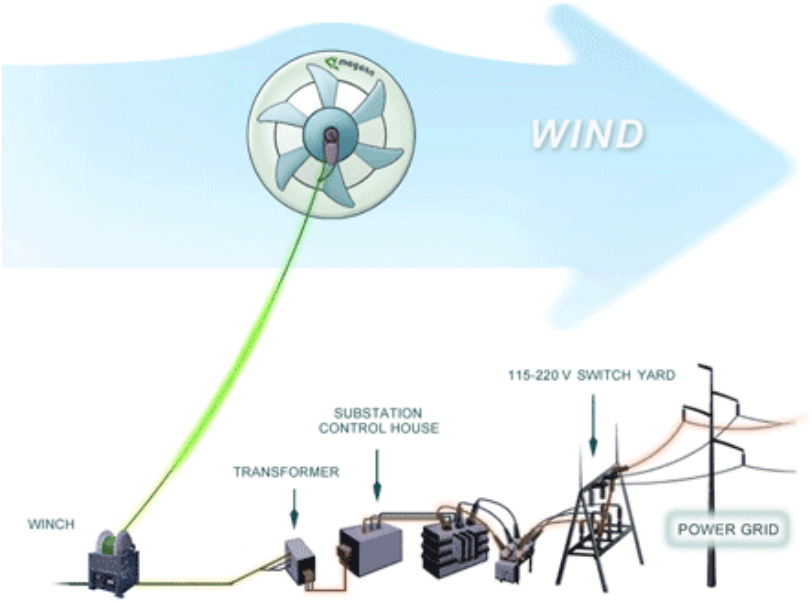

Figure 3.4 - Illustration of the process of produce electric energy by MARS. Retrieved from [9].

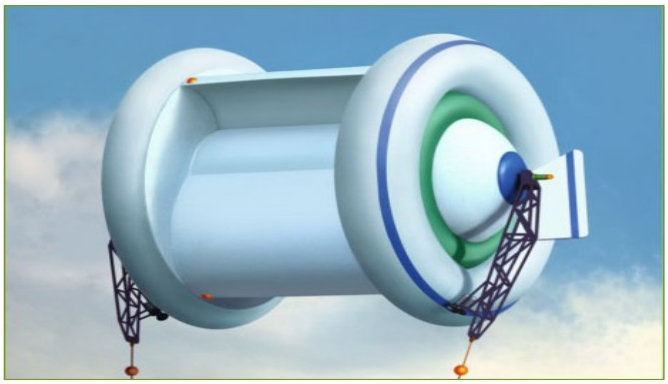

Figure 3.5 – MARS project. Retrieved from [9].

4. Structure of Boreas prototype

The tendencies for future solutions of wind energy production, in opposition to actual wind systems, are constituted by aero structures, lighter than air. In this way the system, which is described, is an aero structure that work in cycles of high altitudes (more than 500 meters) being connected to a capstan on the ground. This system is coupled to an electric generator, producing energy during a part of cycle. The cycle consists of two phases, one productive; where the aero module is lifted pulling the cable that drives a mechanical system that in turn drives a generator. On a second phase, the module comes down by the rewinding the using generator that in this cycle is wired to work as an electric engine. Special clutch arrangement will be needed in order to change in the mechanical actions.

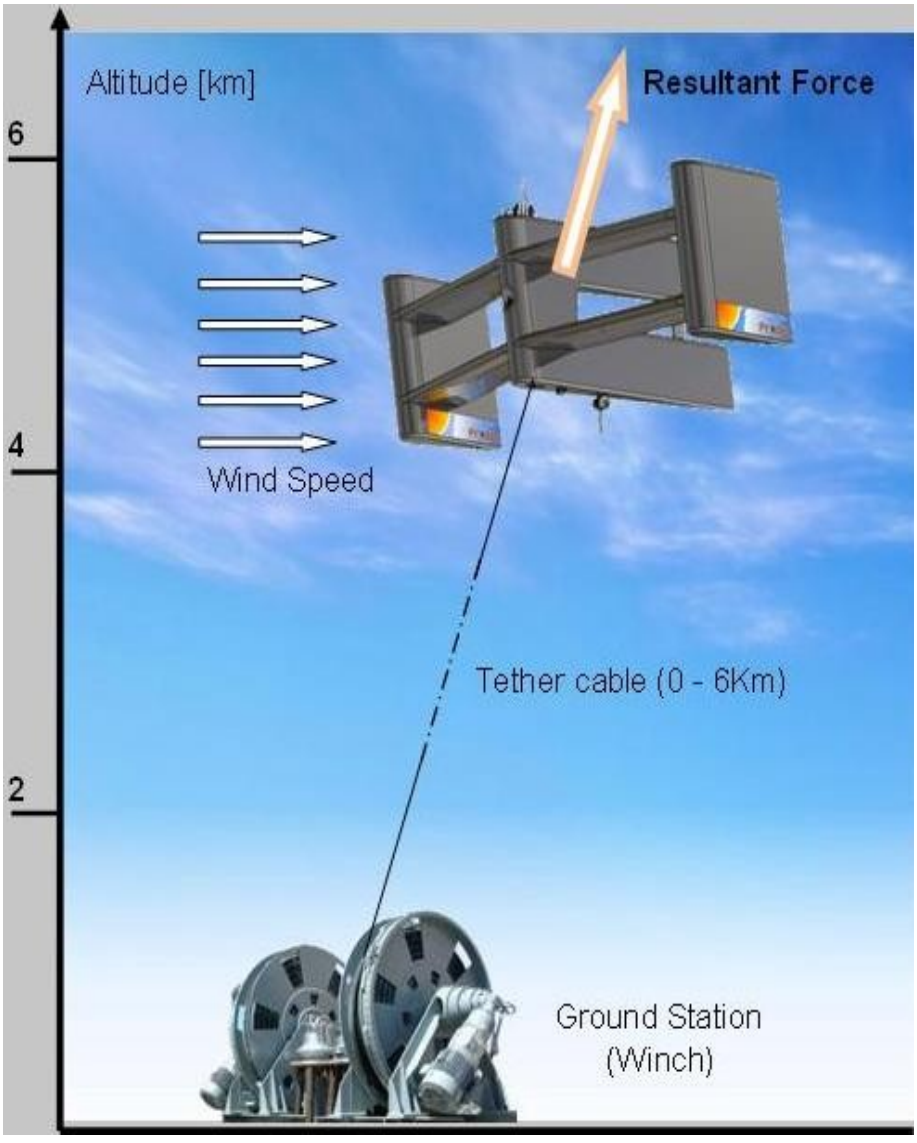

Figure 4.1 - Illustration of Boreas prototype.

4.1. Specifications produced by OMNIDEA

The initial specifications produced by OMNIDEA established the following items:

- Length of cable: 750 (m);
- Typical height range of operation: 150-450 (m);
- Angle typical operation of cable (surface-winch-module air): 40 to 60 degrees;
- Maximum power on unwinding: 120 (kW) (typical situation of speed of unwinding 4 (m/s), tension (30000 (N));
- Maximum tension and speed on unwinding: 50000 (N) and 6 m/s (not simultaneous);
- Maximum power on winding: 80 (kW) (typical situation of speed of unwinding 8 (m/s), tension (10000 (N));
- Maximum tension and speed on winding: 20000 (N) and 12 (m/s), (not simultaneous);
- Lifecycle of equipment: 20 years (more than 1000 000 cycles);
- System must be transportable in a TIR container standard;
- The cable section should be circular and allow the accommodation of gas tubes and electric cables.

4.2. Description of mechanical components of the ground station

The mechanical components of the ground station contain the main items represented on Figure 4.2.

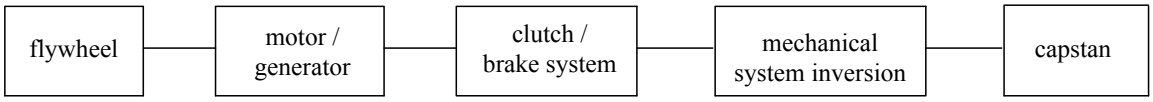

Figure 4.2 - Schematic representation of the components of the system.

On the unwinding cycle the system is coupled, producing energy. The winding begins with the uncoupling the shaft of capstan and the shaft of generator, by the clutch, and then the brake system is actuated to immobilize the capstan. Completed this operation, the mechanical system inversion reverses the rotation of capstan and during the period of time that the capstan needs to reach the rated speed, the flywheel will provide the needed energy. In this way a high pulse of electricity consumption by the system is avoided. Achieved the nominal speed the motor/generator switches to the motor mode (mode power consumption).

Finishing the winding cycle, the clutch is again actuated in order to uncouple the shaft of capstan and shaft of motor; the brake is actuated again in order to immobilize the capstan. The mechanical system inversion reverses the rotation of capstan and its shaft is again coupled with shaft of motor and for then, the motor switches to generator mode.

The system needs also a winding drum to store the cable. All these components must be anchored to the ground and must have the capability of rotation to orient adequately the cable as the wind direction varies.

5. Dimensioning the main mechanical components of ground station of Boreas prototype

On this chapter is proposed the methodology of dimensioning the equipment of system that the development of system should have. Some assumptions are done because is difficult to know exactly some project parameters due to impossibility of test the system. The following considerations are related to the main mechanical components of ground station of prototype.

5.1. Energy considerations

The energy generated during unwinding can be written by (5.1).

$$En = P \times t \tag{5.1}$$

Assuming constant speed, the time is given by (5.2).

$$t = \frac{l_1}{v} \tag{5.2}$$

Take into account the specifications of the device for a typical situation, the specifications of energy are presented on Table 5.1.

Table 5.1 – Energy specifications for a typical situation.

Cycle	P (kW)	l_1 (m)	v (m/s)	t (s)	En (kJ)
Winding	80	500	8	62.5	5000
Unwinding	120	500	4	125	15000

5.2. Energy behaviour of system

For both cycles, the energy has two regimes: transient and stationary taking into account parameters as the lift force or the inertia of system.

In the end of winding cycle, the system already rewound the totality of the cable in operation, so the system will reverse the movement and the nominal force on capstan to unwind should be 30 000 (N), in order to produce 15000 (kJ) of useful energy. The transition between coupling shaft capstan to the motor will produce an overshoot of force, beyond the required one as shown on the Figure 5.1. The maximum value depends on the characteristics of the mechanical system.

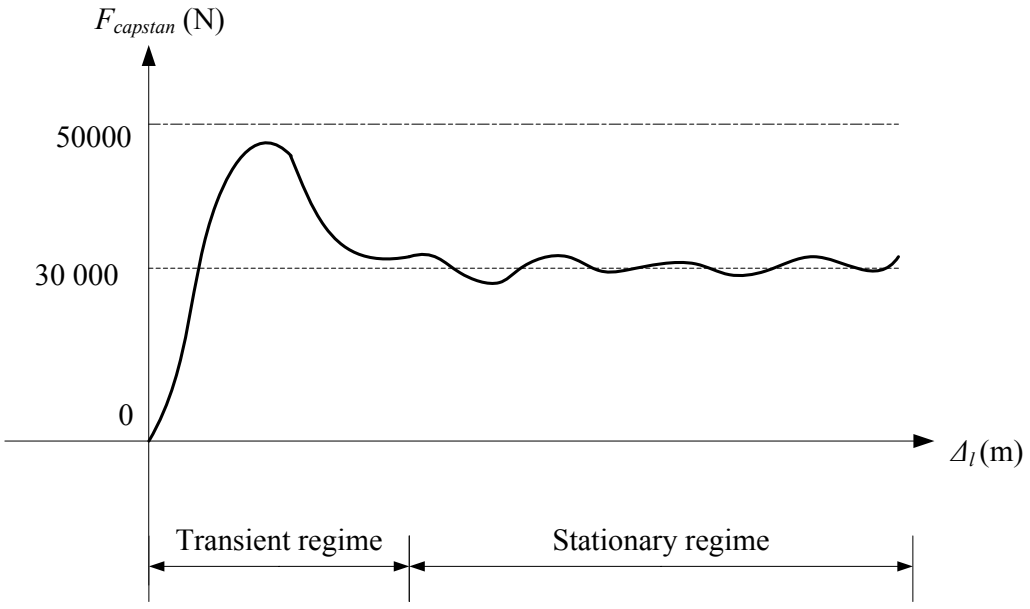

Figure 5.1 - Possible behaviour between the force on capstan and the cable length increment on the unwinding cycle.

At the end of unwinding cycle ends, the motor will be uncoupled from capstan, which is locked and rotation of capstan is reversed. The flywheel will provide power to the motor during a certain period of time, so that it reaches the nominal winding speed (until the nominal force of rewinding reaches nearly 10 000 (N)). Again a transient regime will occur as shown on Figure 5.2. In the same manner, the overshoot will depend from the characteristics of system.

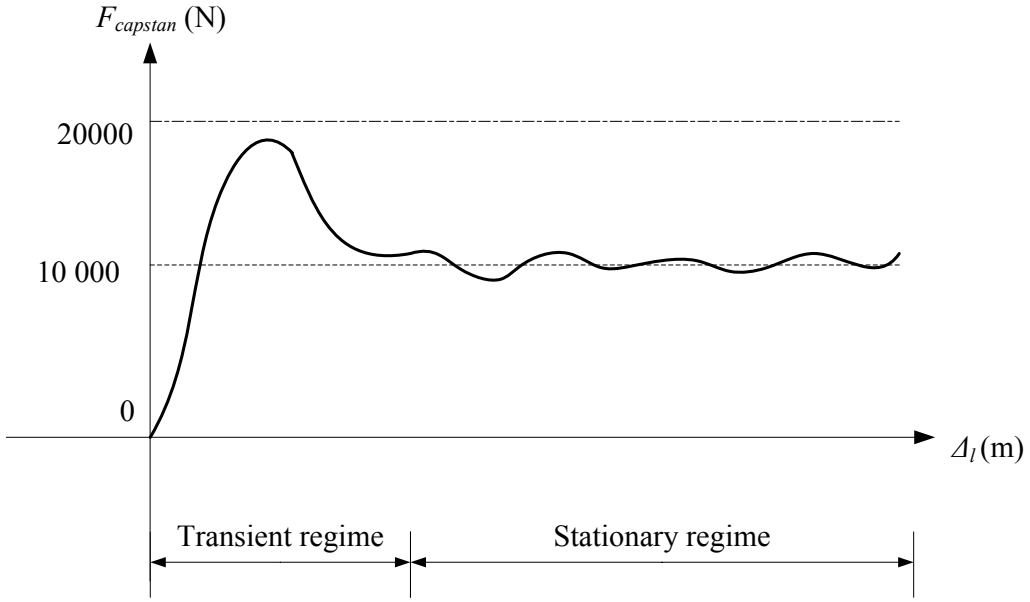

Figure 5.2 - Possible behaviour between the force on capstan and the cable length increment on the winding cycle.

The stored energy, it should be added the resultant energy of losing rotation speed of flywheel after the stabilization of system due the loose by friction, among other factors. For the purposes of this preliminary study it is assumed that about 10% of the total energy to accumulate. It is also assumed that efficiency of electric generator to convert kinematic energy into electric energy is about 95% and therefore an increase of 5% to nominal value.

Table 5.2 - Value of energy to be stored.

En_s (kJ)	En_l (kJ)	η	En_{se} (kJ)
750	75	0.95	862.5

The value of energy is stored on unwinding cycle is 862.5 (kJ). To ensure this value should be taken into account that the nominal speed of unwinding is 4 (m/s). It is assumed that the radius of shaft transmitter power is 150 (mm).

5.3. Dimensioning the flywheel

The value of kinetic energy of flywheel that should be accumulated is given by (5.3):

$$E_{flywheel} = \frac{1}{2} \times I \times {\omega_{motor}}^2 \tag{5.3}$$

So the inertia moment of flywheel is obtained by (5.4).

$$I = 2 \times \frac{E_{flywheel}}{{\omega_{motor}}^2} \tag{5.4}$$

The angular speed ω_{motor} is related to the angular speed of engine which is assumed 1500 (rpm).

Table 5.3 - Considerations to the calculus of inertia moment.

$r_{capstan}$ (m)	ω_{motor} (rad/s)	$E_{flywheel}$ (kJ)	I (kg m^2)
0.325 (*)	157.080	862.5	69.911

The inertia moment for hollow cylinder is described by (5.5).

$$I = \frac{1}{2} \times \pi \times \rho_{flywheel} \times t_{h\text{flywheel}} \times \left({r_{cylinder2}}^2 + {r_{cylinder1}}^2 \right) \tag{5.5}$$

In order to achieve the value of inertia moment, geometry of flywheel is proposed of Figure 5.3.

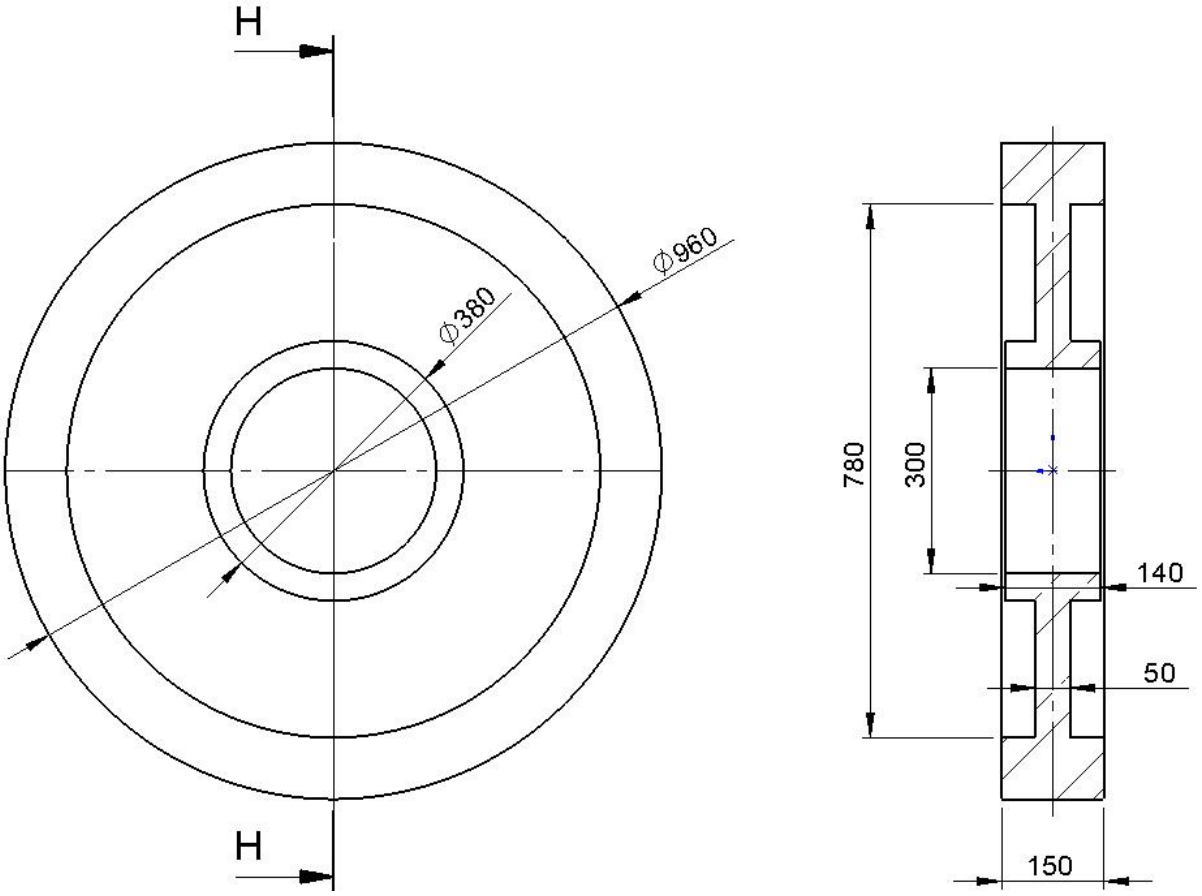

Figure 5.3 – Flywheel approximate dimensions.

5.4. Dimensioning the cable

This topic is related to specification the section of cable take into account that the cross section is not available.

5.4.1. Initial considerations

The determination of the normal stress that the cable can have during the cycles of operation is brought by (5.6).

$$\sigma_{Service} = \frac{F_{max}}{\Omega} \tag{5.6}$$

The determination of ultimate stress is given by (5.7).

$$\sigma_{Ultimate1} = \frac{MBF}{\Omega} \tag{5.7}$$

The maximum allowable stress is obtained by (5.8).

$$\sigma_{allowable1} = \frac{\sigma_{Ultimate1}}{Sf_1} \tag{5.8}$$

According to the specifications, the maximum tension of service on cable is 50000 (N). The manufacturer of cable, EURONEEMA, specifies the MBF for a certain value of external surrounding diameter. The chosen value for Sf_1 is 3. The characteristics of cable and the variables to the determine the maximum allowable stress are presented on Table 5.4.

Table 5.4 - Value of maximum allowed stress on the cable. Adapted from [10**].**

d (m) [10^{-3}]	Ω (m^2) [10^{-4}]	Weight (kg/100 m)	MBF (kN)	F_{max} (kN)	$\sigma_{Service}$ (MPa)	$\sigma_{allowable1}$ (MPa)
6	0.283	2.2	35	50	1768.659	412.687
8	0.503	4	62	50	994.629	411.113
10	0.785	6	97	50	636.618	411.680
12	1.131	9.3	137	50	442.087	403.772
14	1.539	10.7	184	50	324.886	398.527
16	2.011	15	244	50	248.633	404.442
18	2.545	19.6	303	50	196.464	396.857
20	3.142	23.1	374	50	159.134	396.775

The areas expressed in Table 5.4 refer to filled sections, although the section of cable expected to be implemented, is a combination of elliptical coils that have voids between them. It would be necessary to analyse several samples from different sections of cable in order to determinate a medium value of area. The material of the cable is UHMPE with commercial name of EURONEEMA.

Figure 5.4 - Sample of cable expected to be use. Retrieved from [10].

The value of area is related to a diameter of 14 (mm) because in this section the service stress is the nearest of the respective maximum allowable stress.

The project requires that the cable has a structural hollows section to allow the passage of electric cable and gas tubes. The section houses an electrical cable with 8 (mm) of diameter, housed in the inner section and two gas pipes with a thickness of 4 (mm) being the inner diameter, D_{int}, of 12.2 (mm). Considering the structural cable, the section of cable has geometry of a ring represented on Figure 5.5.

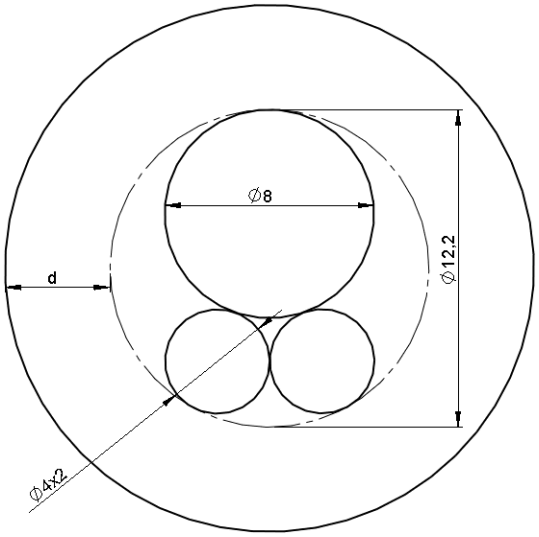

Figure 5.5 - Section of a structural cable with an electric cable and two tubes of gas.

The external diameter of the ring, D_{ext},, takes into account D_{int} and the diameter of structural cable d, being expressed by (5.9).

$$D_{ext} = D_{int} + 2d \tag{5.9}$$

In this way the area is obtained by (5.10).

$$\Omega = \pi \times \left(\frac{{D_{ext}}^2 - {D_{int}}^2}{4}\right) \quad (5.10)$$

5.4.2. Determination of structural cable diameter

In order to determinate Ω, a 3 (mm) structural cable is tested, being the results on Table 5.5.

Table 5.5 – Variables to determinate Ω for a d value of 3 (mm).

D_{int} (m) [10^{-3}]	d (m) [10^{-3}]	D_{ext} (m) [10^{-3}]	Ω (m^2) [10^{-4}]
12.2	3	18.2	1.433

For inner diameter, with 12.2 (mm), and a structural cable with 3 (mm) of diameter displayed on a ring, the area is less than the reference area value, $1.539 \times 10^{-4} (m^2)$. In this way a ring with the referred inner diameter, with a structural cable of 4 (mm), will be evaluated, being the results on Table 5.6

Table 5.6 - Variables to determinate Ω for $d$value of 4 (mm).

D_{int} (m) [10^{-3}]	d (m) [10^{-3}]	D_{ext} (m) [10^{-3}]	Ω (m^2) [10^{-4}]
12.2	4	20.2	2.036

For a ring with 4 (mm) of thickness, and an inner diameter of 20.2 (mm) the value of area is higher than the reference value, so the condition is validated.

5.4.2.1. Determination of the weight of the different cables

In this topic the weight of structural cable, electrical cable and gas tubes are proposed.

5.4.2.1.1. Weight of structural cable unit of length

From the Table 5.4, the weight of structural cable can be estimated by the following relation:

$$1{,}539 \times 10^{-4}\ m^2 \ \rightarrow 0.107 \text{ (kg/m)}$$
$$2{,}033 \times 10^{-4}\ m^2 \ \rightarrow W_{sc} \text{ (kg/m)}$$

So the value of W_{sc} is:

$$W_{sc} = 0{,}141 \text{ (kg/m)}$$

The transformation of weight of structural cable in kg/m to N/m is given by (5.11).

$$W_{sc}(N/m) = W_{sc}(\ k_g/m) \times g$$

$$W_{sc} = 0.141\ \times 9.807 = 1.383\ \text{(N/m)} \tag{5.11}$$

5.4.2.1.2. Weight of electric cable for unit of length

The weight of the electric cable for unit of length is given by (5.12).

$$W_{ec} = \rho_{copper}\ \times V_{ec} \times g \tag{5.12}$$

The value of V_{ec} is given by (5.13).

$$V_{ec} = \pi \times \frac{{D_{ec}}^2}{4} \times 1 \tag{5.13}$$

Take into account the considerations; it obtains a value of W_{ec} shown on Table 5.7.

Table 5.7 - Variables to determinate W_{ec}.

D_{ec} (m) [10^{-3}]	ρ_{copper} (kg /m^3)	g (m s^{-2})	V_{ec} (m^2) [10^{-5}]	W_{ec} (kg /m)	W_{ec} (N/m)
8	8910, [**11**]	9.807	5.027	0.448	4.393

5.4.2.1.3. Weight of gas tube for unit of length

The weight of gas tube for unit of length is obtained by (5.14).

$$W_{gt} = \rho_{\text{polyamide}} \times V_{gt} \times g \tag{5.14}$$

The value of V_{gt} is given by (5.15).

$$V_{gt} = \pi \times \left(\frac{{D_{extg}}^2 - {D_{intg}}^2}{4}\right) \times 1 \tag{5.15}$$

Take into account the considerations; it obtains a value of W_{gt} shown on Table 5.8.

Table 5.8 - Variables to determinate W_{gt}.

D_{extg} (m) [10^{-3}]	D_{intg} (m) [10^{-3}]	$\rho_{\text{polyamide}}$ (kg /m^3)	V_{gt} (m^2) [10^{-6}]	W_{gt} (kg/m) [10^{-3}]	W_{gt} (N/m) [10^{-2}]
4	2.7	1400, [**12**]	6.841	9.577	9.393

This weight must be multiply by 2, because there are two tubes. So:

Table 5.9 - Total value of weight of gas tubes.

W_{gt} (kg/m) [10^{-2}]	W_{gt} (N/m)
1.915	0.188

5.4.2.1.4. Total weight of cable

The total weight of cable is given by (5.16) being the results on Table 5.10.

$$W_{cable} = W_{sc} + W_{ec} + W_{gt} \tag{5.16}$$

Table 5.10 - Weight of cable and of the different components.

W_{sc} (kg /m)	W_{gt} (kg /m) [10^{-2}]	W_{ec} (kg/m)	W_{cable} (kg /m)	W_{cable} (N/m)
0.141	1.915	0.448	0.608	5.963

5.4.3. Real cross section of cable

The cable is a combination of sections that on a first assumption are considered as circulars, existing interstices (voids) between them so it is necessary verify which is the effective area, considering an outer diameter of 20.2 (mm).

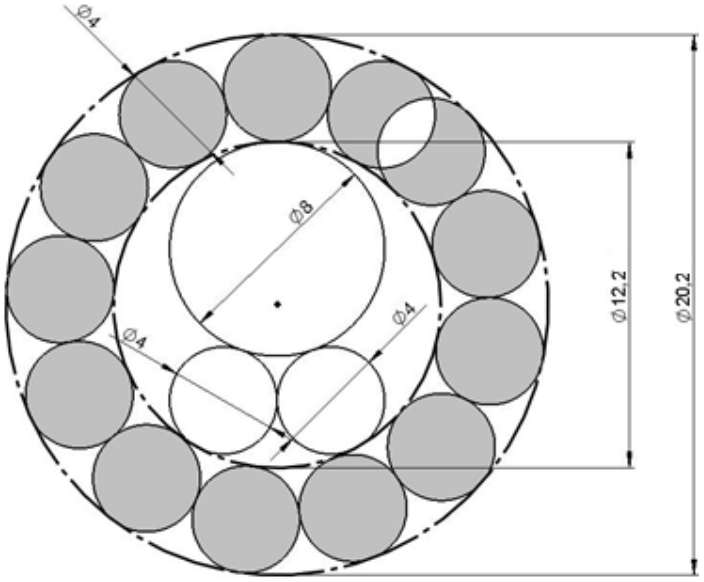

Figure 5.6 – Illustration of the area for a structural cable of 4mm diameter.

A structural cable with circumferences of 4 (mm), has a value of area, Ω, of 1.557×10^{-4} (m^2), which is bigger than the reference value , 1.539×10^{-4} (m^2). So the area of reference is checked.

Considering that the space occupied by ellipses in the ring is greater than circumferences, it is estimated that the area is higher than the actual resistance value of a structural cable with circumferences of 4 (mm). So it will be used the value of area of 1.539×10^{-4} (m^2), with the weight of cable of 5.963 (N/m), knowing that these values are not overestimated on a large scale.

5.5. Dimensioning the capstan drum

On this topic the dimensions of capstan drum is proposed and verified to the loads.

5.5.1. Non-rotating thick cylinder

Assuming the model of thick cylinder submitted to pressure, the study is based on a static approach. The procedure developed elsewhere [**13**] is used. Further details can be obtained there.

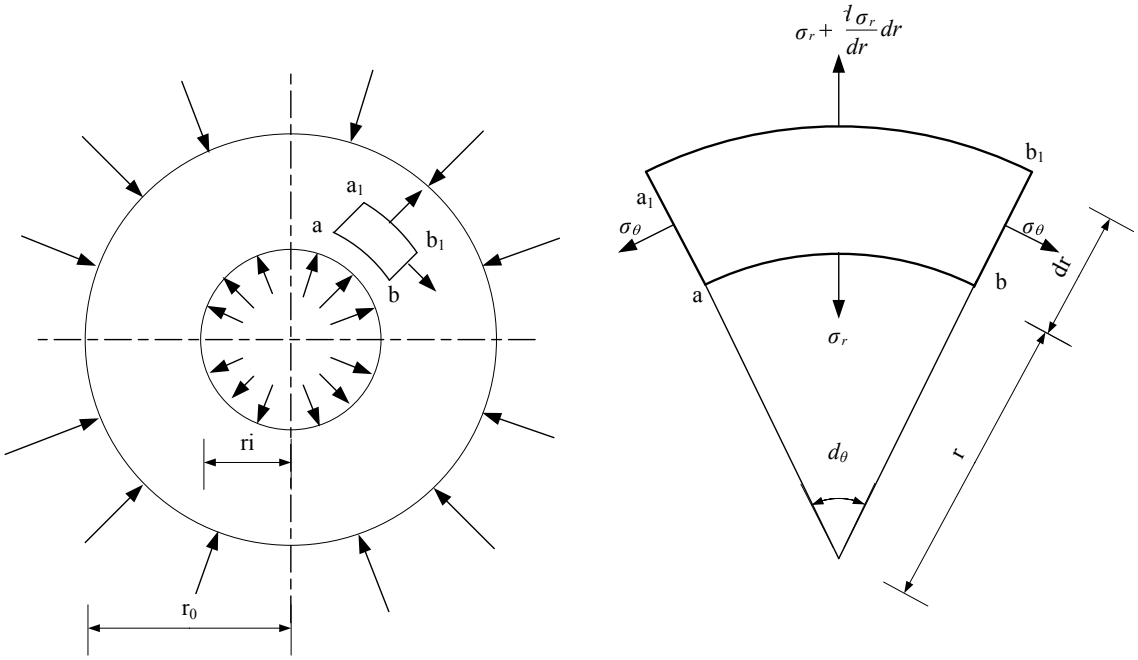

Figure 5.7 –Forces acting on a general element in a rotating disc. Adapted from [13**].**

A constant thick cylinder thickness, where acting internal and external pressures distributed on a uniform way. The deformation is symmetric relatively to the cylinder axis and his value don´t vary at the length of cylinder.

An element of the cylinder ab-a1b1, Figure 5.7, with unitary thickness that for symmetric reason will not occur shear stress on the focus of the selected element. The σ_θ is the tangential stress normal to faces aa1 e bb1 and σ_r be the radial stress normal to ab face. This stress is function of r and vary $\frac{d\sigma_r}{dr}$.

The sum of the projections of forces based on the bisector of angle d_θ, not considering the self weight, gives the equilibrium equation (5.17).

$$\sigma_r r\, d\theta + \sigma_\theta r\, d\theta - \left(\sigma_r + \frac{d\sigma_r}{dr}\, dr\right)(r + dr) \times d\theta \tag{5.17}$$

If the higher order infinitesimals were neglected, obtains the equation (5.18).

$$\sigma_\theta - \sigma_r - r\left(\frac{d\sigma_r}{dr}\right) = 0 \tag{5.18}$$

The deformation on the cylinder is symmetric and a radial displacement of all points of the wall is the same. The deformation is constant on the circumferential direction, but varies radially. If u is the displacement of the cylindrical surface of radius r, for the surface of radius $r + dr$, the displacement is given by (5.19)

$$u + \frac{du}{dr} dr \tag{5.19}$$

The unit radial strain is brought by (5.20).

$$\varepsilon_r = \frac{u + \frac{du}{dr} dr - u}{dr} = \frac{du}{dr} \tag{5.20}$$

The unit tangential strain is given by (5.21).

$$\varepsilon_t = \frac{\mathrm{u}}{\mathrm{r}} \tag{5.21}$$

In this way the stress equations can be written by the equation (5.22).

$$\begin{cases} \sigma_r = \frac{\mathrm{E}}{1-\mu^2}\left(\frac{\mathrm{du}}{\mathrm{dr}} + \mu \times \frac{\mathrm{u}}{\mathrm{r}}\right) \\ \sigma_\theta = \frac{\mathrm{E}}{1-\mu^2}\left(\frac{\mathrm{u}}{\mathrm{r}} + \mu \times \frac{\mathrm{du}}{\mathrm{r}}\right) \end{cases} \tag{5.22}$$

If these values be substituted on the equilibrium equation, the result is the following differential equation (5.23).

$$\frac{d^2 r}{dr^2} + \frac{1}{r} \times \frac{\mathrm{du}}{\mathrm{dr}} - \frac{\mathrm{u}}{\mathrm{r}^2} = 0 \tag{5.23}$$

The general solution is given by (5.24).

$$u = c_1 r + \frac{c_2}{r} \tag{5.24}$$

So it obtains the equations (5.25) and (5.26).

$$\sigma_r = \frac{E}{1-\mu^2}\left[c_1(1+\mu) - c_2\left(\frac{1-\mu}{r^2}\right)\right] \tag{5.25}$$

$$\sigma_\theta = \frac{E}{1-\mu^2}\left[c_1(1+\mu) + c_2\left(\frac{1-\mu}{r^2}\right)\right] \tag{5.26}$$

The constants c_1 and c_2 are determinate by boundary conditions, which refer to the value of external pressure and internal pressure. The value of constants can be written by (5.27) and (5.28).

$$c_1 = \frac{1-\mu}{E} \times \frac{r_i^2 p_i - r_0^2 p_i}{r_0^2 - r_i^2} \tag{5.27}$$

$$c_2 = \frac{1-\mu}{E} \times \frac{r_i^2 r_0^2 (p_i - p_0)}{r_0^2 - r_i^2} \tag{5.28}$$

These expressions when inserted on (5.25) (5.26), allows the achievement of (5.29) and (5.30).

$$\sigma_r = \frac{r_i^2 P_i - r_0^2 P_0}{r_0^2 - r_i^2} - \frac{r_i^2 r_0^2 (p_i - p_0)}{r^2 (r_0^2 - r_i^2)} \tag{5.29}$$

$$\sigma_\theta = \frac{r_i^2 P_i - r_0^2 P_0}{r_0^2 - r_i^2} + \frac{r_i^2 r_0^2 (p_i - p_0)}{r^2 (r_0^2 - r_i^2)} \tag{5.30}$$

The value of σ_r+σ_θ is constant and the deformation is the same for all the elements, so planar sections remains planar after the deformation. For the particular case, p_i is 0 which means that the internal pressure is 0, so it finally obtains the equations (5.31) and (5.32).

$$\sigma_r = \frac{P_0 \times r_0^2}{r_0^2 - r_i^2} \times \left(1 - \frac{r_i^2}{r^2}\right) \tag{5.31}$$

$$\sigma_\theta = \frac{P_0 \times {r_0}^2}{{r_0}^2 - {r_i}^2} \times \left(1 + \frac{{r_i}^2}{r^2}\right) \quad (5.32)$$

The value of σ_r is maximum for $r = r_0$, σ_θ is maximum for $r = r_i$, $\sigma_\theta > \sigma_r$ and these stresses are always compressive stresses.

5.5.2. Rotating thick cylinder

A thin thick-walled cylinder with constant thickness, with an outer radius r_2, an inner radius r_1 in rotation with a constant angular speed ω, with a density ρ and a Possion´s ratio μ, has a tangential stress, [**14**]:

$$\sigma_\theta = \frac{(3+\mu) \times \rho_{steel} \times \omega^2}{8} \times \left[{r_{capstan}}^2 - \frac{1+3\mu}{3+\mu} r^2 + {r_{capstani}}^2 \left(1 + \frac{{r_{capstan}}^2}{r^2}\right)\right] \quad (5.33)$$

5.5.3. Pressure on the capstan drum

The pressure applied by the cable into the drum of capstan can be determinate if we consider one half of drum, being the equilibrium given by (5.34).

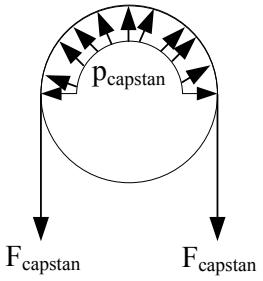

Figure 5.8 - Pressure diagram on capstan. Adapted from [13**].**

$$2F_{capstan} = p_{capstan} \times \int_0^\pi r_{capstan} d\beta \quad (5.34)$$

Solving equation (5.34), it is obtained the expression (5.35).

$$p_{capstan} = \frac{4F_{capstan}}{\pi D_{capstan} d} \quad (5.35)$$

The length of capstan depends from number of turns that the capstan drum can have. So the number of turns take into account the relation of $F_{capstan}$, the load side, and tension that goes to winder drum, F_{winder}, hold side, being brought it by (5.36).

$$F_{capstan} = F_{winder} \times e^{\gamma \phi_2} \tag{5.36}$$

Establishing a relation R, between $F_{capstan}$ and F_{winder} the value of ϕ_2 is given by (5.37)

$$\phi_2 = \frac{ln(R)}{\gamma} \tag{5.37}$$

The length of capstan drum depends from number of turns that the capstan drum can have, and the external diameter of cable, being given by (5.38).

$$L = \frac{\phi_2 \times D_{ext}}{2\pi} \tag{5.38}$$

Bearing in mind that the quotient between the diameter of capstan and diameter of cable should, at least, be equal or greater than 30, according to manufacturer of cable (LANKHORST EURONETE ROPES, S.A.), so a diameter of capstan of 650 (mm) is chosen.

Table 5.11 - Variables to determine the external pressure and length of capstan.

$F_{capstan}$ (N)	γ	R (m)	ϕ_2 (rad)	Nº of spires	d (m)	D_{ext} (m)	$D_{capstan}$ (m)	L (m)
50000	0.1	10	69.078	11	0.0041	0.0202	0.65	0.222

Sizing the capstan with one more spire, with 4 (mm) of spacing between the spires and a margin of 20 (mm) flanges on each side until the flanges result on a length of capstan of 331.7 (mm).

5.5.4. Results

Considering a non-rotating cylinder the results are expressed on Table 5.12.

Table 5.12 - Maximum and minimum values of the radial and tangential stress on the drum of capstan considering a non-rotating cylinder.

	σ_r (MPa)	σ_θ (MPa)
r_i	0	-172.415
r_0	-24.485	-147.930

Considering rotation on the cylinder the tangential stress is expressed on Table 5.13.

Table 5.13 - Maximum and minimum values of the tangential stress on the drum of capstan considering a rotating cylinder.

	σ_θ (Mpa)
r_i	-172.296
r_0	-172.319

So the maximum value of tangential stress of compression of 172.415 (MPa). The maximum allowable stress of capstan is obtained by (5.39).

$$\sigma_{allowable2} = \frac{\sigma_{Ultimate2}}{Sf_2} \tag{5.39}$$

The material, ultimate stress the safety of factor chosen, admit the maximum allowable stress on capstan, expressed on Table 5.14.

Table 5.14 - Variables to determine the maximum allowable stress on capstan.

Designation	$\sigma_{Ultimate2}$ (MPa)	Sf_2	$\sigma_{allowable2}$ (MPa)
Steel (S355), [**11**]	355, [**11**]	2	177.5

The values of $\sigma_{allowablec}$ and σ_θ, allow a thickness on capstan drum presented on Table 5.15.

Table 5.15 - Maximum allowable stress, tangential stress and thickness of capstan.

$\sigma_{allowable2}$ (MPa)	σ_{θ} (Mpa)	$t_{hcapstan}$ (mm)
177.5	-172.415	50

The dimensions of capstan are illustrated on Figure 5.9.

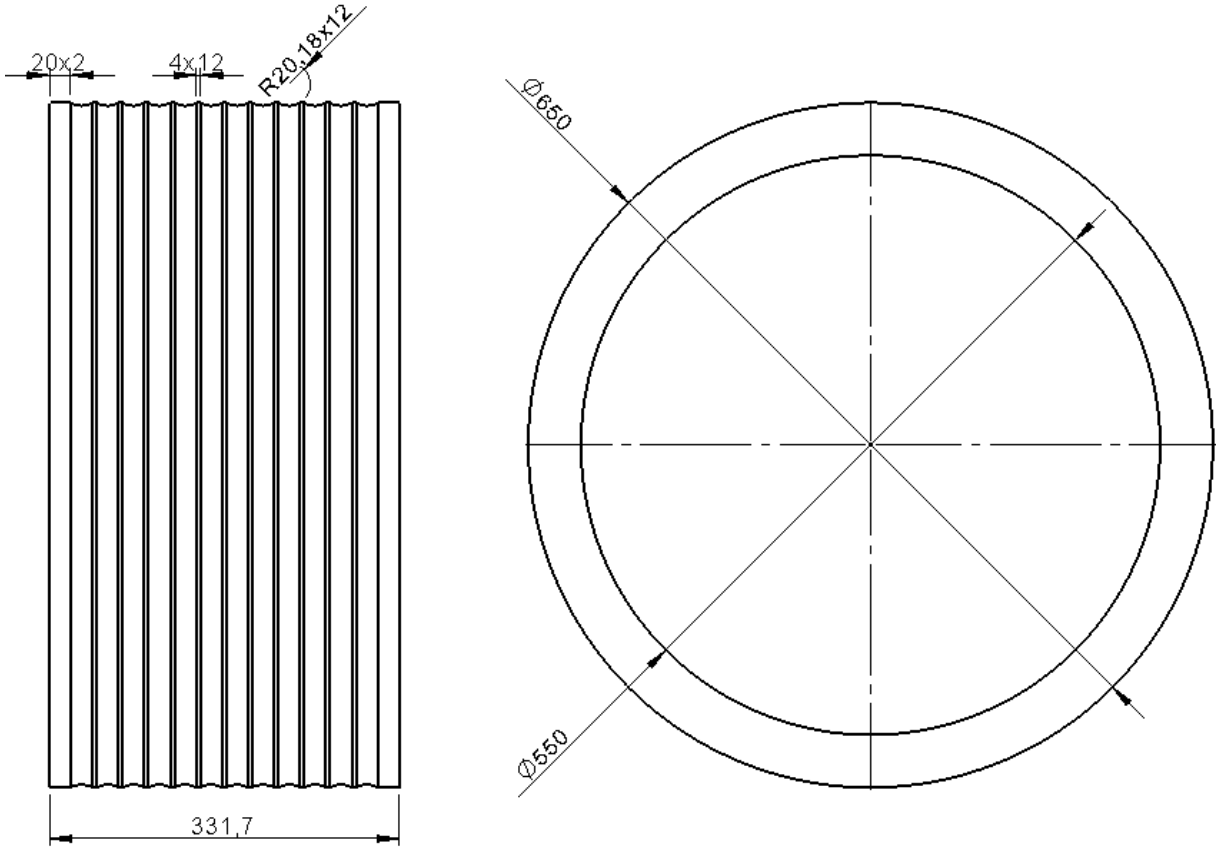

Figure 5.9 - Dimensions of drum of capstan.

5.6. Dimensioning the winder drum

In order to determinate the radius of drum, the total length of cable is an important parameter, shown on obtained by (5.40), and shown on Figure 5.10.

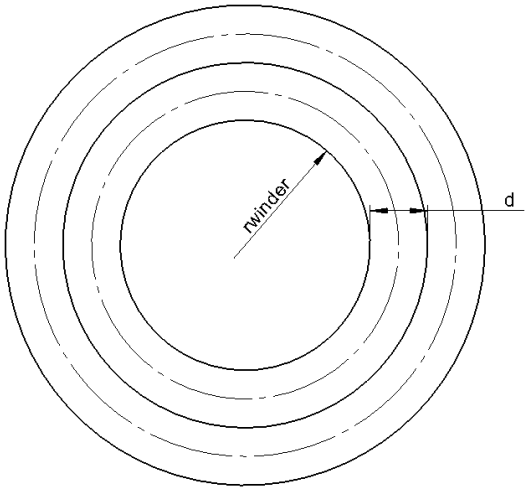

Figure 5.10 - Illustration of cable length for a certain loop.

$$r_i = r_{winder} + ((i-1) * d) + \frac{d}{2} \tag{5.40}$$

The length of cable for a certain loop is given by (5.41).

$$l_i = \sum_1^i 2 \times \pi \times r_i \times S \tag{5.41}$$

The value of *S* is given by (5.42).

$$S = \frac{L\ winder}{d} \tag{5.42}$$

The total length of cable is given take into account the length of cable on a certain loop and is given by (5.43):

$$L_t = \sum_1^i l_i \tag{5.43}$$

The diameter of flanges is given by (5.44).

$$D_{flange} = 2 \times (N \times D_{ext}) + 2 \times r_{winder} \tag{5.44}$$

Taking into account that the total of length of cable is 750 m, the parameters where adjusted in order to reach a value of length of cable near the reference value.

Table 5.16 - Geometric characteristics of winder.

r_{winder} (m)	D_{ext} (m) [10^{-3}]	L_{winder} (m)	N	S	D_{flange} (m)
0.4	20.2	0.75	7	38	1.083

The model of shell (curve plate of thin wall), by membrane theory, can be used. It is assumed:

- Stresses are constant on the thickness of shell;
- The quotient between the thickness/radius of curvature is less than 1/20;
- There is a stress plain (two principal stress);
- Low deformations, the bigger deformation is less than half of the thickness of shape;
- Secondary stresses are not evaluated.

For a cylindrical shell, the tangential stress, also called hoop stress, is given by (5.45), [**11**].

$$\sigma_{\theta 1} = \frac{p_{winder} \times \mathrm{r_{int}}}{t_{hwinder}} \tag{5.45}$$

Due the rotation of the winder, another tangential stress is given by (5.46), [**15**].

$$\sigma_{\theta 2} = \rho \omega^2 {r_{int}}^2 \tag{5.46}$$

The total tangential stress is given by (5.47).

$$\sigma_1 = \sigma_{\theta 1} + \sigma_{\theta 2} \tag{5.47}$$

Using the Tresca criterion, this leads to (5.48).

$$\sigma_1 - \sigma_3 \leq \sigma_{allowablew} \tag{5.48}$$

Considering plane stress, σ_3=0, therefore (5.49).

$$\sigma_1 \leq \sigma_{allowable3} \tag{5.49}$$

The value of p_{winder} for different spires of winding can be approximate to (5.50) , [**16**].

$$p_{winder} = s(r_{windermed}) - \int_{r=r_{winderint}}^{r=r_{winderext}} s(r_{windermed}) \frac{r_{windermed}}{r^2 - {r_{winderint}}^2} \left(1 + \frac{{r_{winderext}}^2}{r_{windermed}}\right) dr_{windermed} \tag{5.50}$$

The value of $r_{winderext}$, is given by (5.51).

$$r_{winderext} = r_{winderint} - t_{hwinder} \tag{5.51}$$

The tension to apply to cable on the winder should be the minimum possible, ideally null, in order to reduce the friction. So the expressions presented represent a methodology for the determination of thickness of winder but have in mind that the tension on cable when goes to winder is low, the thickness of winder is determinate by the manufacturing process. Knowing the lathe process will be used is proposed a value of 30 (mm) to the sheet, that will be curved and then welded.

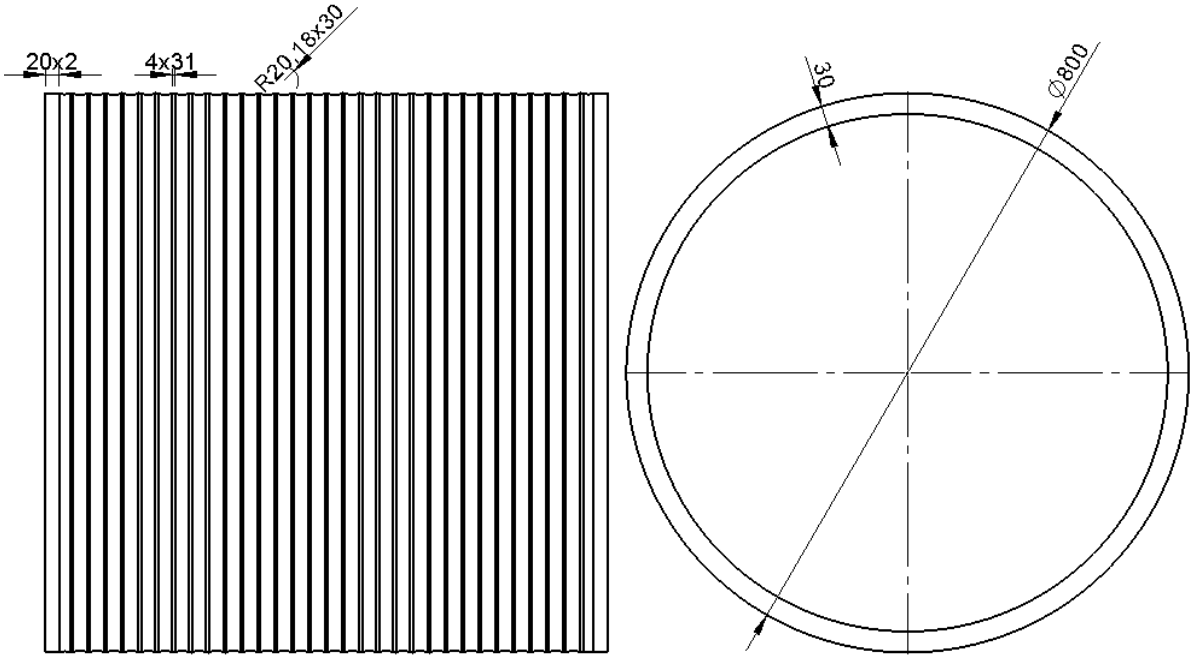

Figure 5.11 - Dimensions of winder drum.

6. Modelling the cable structure

As referred earlier, one of the main objectives of this thesis is the cable modelling, in order to determine the stresses involved and the estimation of trajectory of the cable. In this way, two approaches are exposed in order to give answers to the control of device.

6.1. Analytical equations to study cable structures

Usually the cable structures are analyzed with simplified analytical equations, such as the catenary equation, in which the cable supported on two rigid ends requested by a load uniformly distributed along its axis, such as the self-weight of the cable, [**17**].

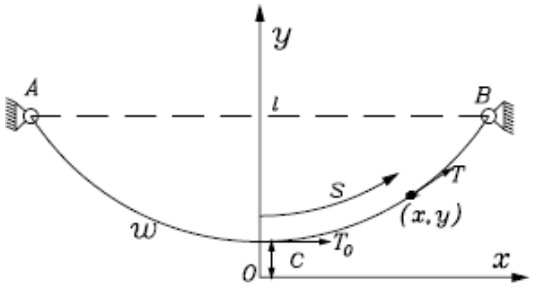

Figure 6.1 - Configuration of equilibrium of catenary. Retrieved from [17**].**

The equations that described the behaviour of catenary are, [**17**]:

$$y = c\cosh\left(\frac{x}{c}\right) \tag{6.1}$$

$$s^2 = y^2 - c^2 \tag{6.2}$$

$$T_0 = c \times W_{catcable} \tag{6.3}$$

$$T = y \times W_{catcable} \tag{6.4}$$

6.2. FEM

The finite element method is a numerical method (approximate method), where the domain of problem is decomposed into several sub domains. In each of these sub domains, the equations that regulate the phenomenon are approximated by a variational method. The approximation of a solution into several sub domains allows an easier representation of a complicated function by a composition of simple polynomials functions where the error can be as small as desired, simply increasing the number of sub domains, [**18**].

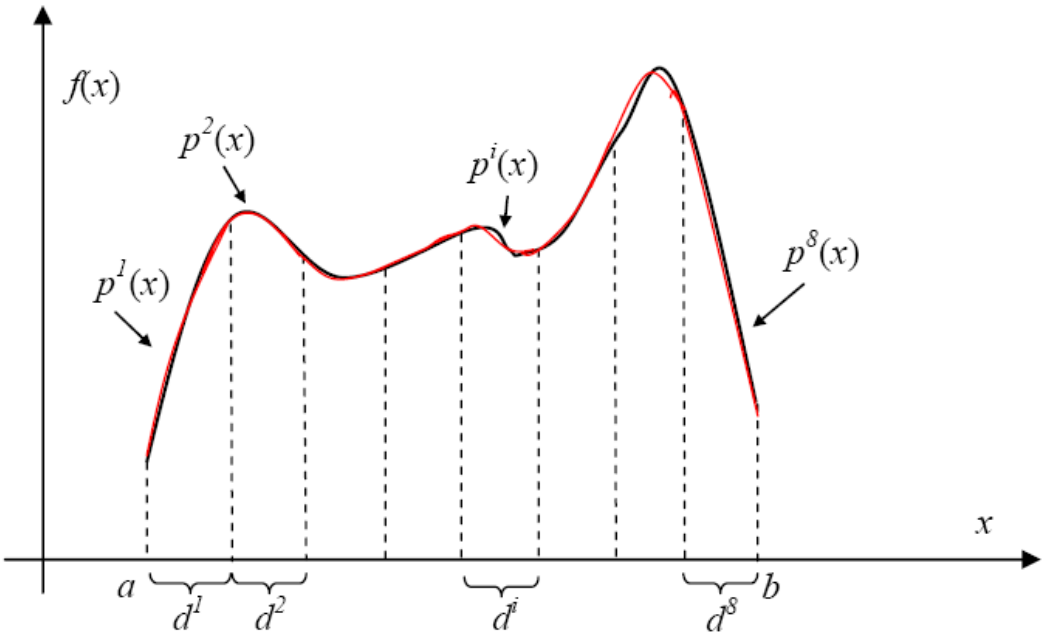

Figure 6.2 - Example of a function *f(x)* approximated by a conjunct of functions $p^i(x)$. Retrieved from [18].

In Figure 6.2 the function, *f(x)* depicted as solid line, is approximated by the polynomials $p^i(x)$, represented at red, ($p^1(x)$, $p^2(x)$... $p^8(x)$). The polynomials are defined on sub domains, d^i, and at the time that the number of sub domains increase, lesser is the error on the approximation.

The FEM requires the utilization of the variational principles (principle of virtual work, the principle of stationary potential energy or the principle of Hamilton, etc) because the problem must be formulated as a defined integral in the whole domain, in other words, the sets of equations that describe the physical phenomena establish relationships between the variables and the parameters of the problem on the neighbourhood of each point, so in order to pass this description of the physical phenomenon to the integral description, it is necessary to use the variational principles, [**18**].

The FEM is a stratified methodology: it can be used to solve one-dimensional problems, but generally is applied to problems where the solution is an area or a generic tri-dimensional volume. In any of these cases the first step is divide on finite number of segments, areas or volumes smaller, called finite elements. This process is the discretization, [**19**]. On the Figure 6.3 is shown the schematic representation of the process of discretization of the domain by finite elements.

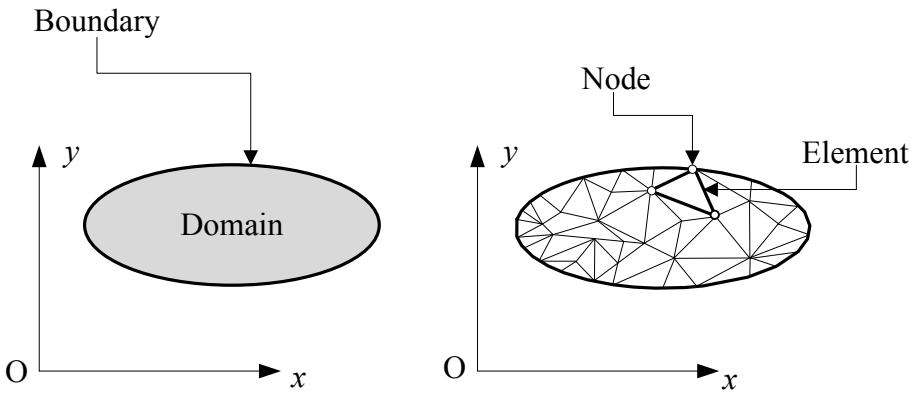

Figure 6.3 - Schematic representation of the process of discretization of the domain by finite elements. Adpated from [19**].**

The finite elements can have different geometric shapes, being one-dimensional, bi-dimensional or tri-dimensional.

To solve one-dimensional problems (or consisting of one-dimensional elements) the finite elements have the shape of segments. On bi-dimensional problems the elements are frequently quadrilaterals or triangles and for tri-dimensional problems the elements can be hexahedral, tetrahedral, pentahedral, etc.

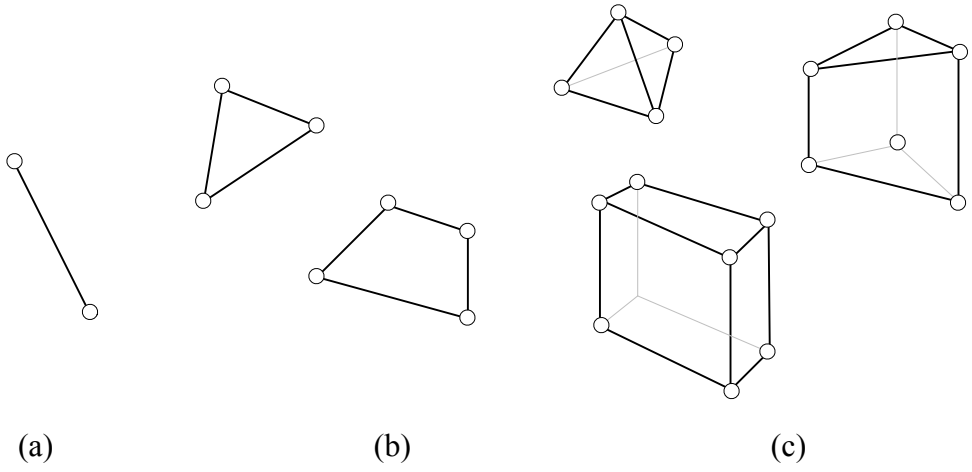

Figure 6.4 - Examples of geometric configurations of finite element. Finite element: a) one-dimensional, (b) bi-dimensional and (c) tri-dimensional. Adapted from [19**].**

Considering a linear elastic analysis of general problems in engineering, usually in FEM the first step is to determine the field of displacements of a finite number of points in system. These points are the nodes of the mesh of finite element, which are on vertex of elements, as it shown on and Figure 6.5. Is important note that depending of the type of formulation in finite element analysis, the nodes can be on the edges, on their faces or inside them. The nodes that belong to the boundary of adjacent elements must be common to all elements that exist there. For this reason is not possible the discretization of a solid medium in elements that do not coincide on their own nodes.

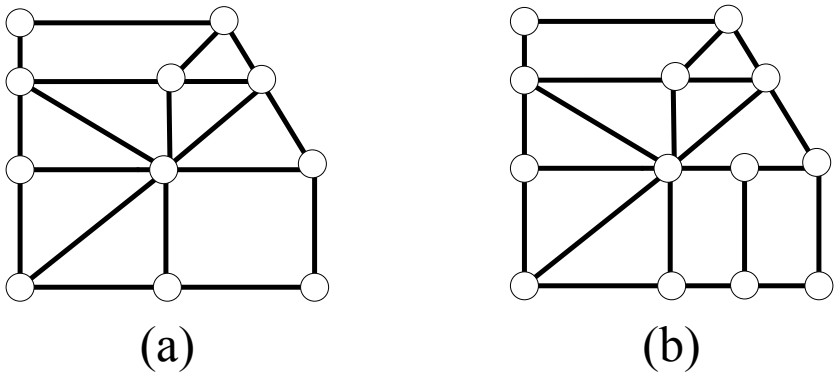

Figure 6.5 - Example of a bi-dimensional mesh of finite elements (a) allowed and (b) not allowed. Adpated from [19**].**

In this way the numerical analysis done with the finite element method, on a first step, calculates the node displacements for a certain load on the domain under analysis. So the displacement of each point of the finite element can be determined by the displacements of

the nodes on that element, which is, according to the nodal displacements. In this way the calculation of the displacements of a finite number of elements (the nodes of the mesh) allows the determination of an infinite number of points of a continuous domain. In other words, the displacement of any point can be defined according the displacements of the nodes of the element that the point belong, [**19**].

For example on a bi-dimensional, the displacement of each node can be decomposed in two perpendicular components, one parallel to a reference axis *Ox* and other parallel to a reference axis *Oy*. These components of displacement are called degrees of freedom. On a bi-dimensional case each node has two degrees of freedom, concerning the axis *Ox* and *Oy*. Analogously for a tri-dimensional finite element each node has three degrees freedom, have in mind the relationship between that point with the three orthogonal spatial directions.

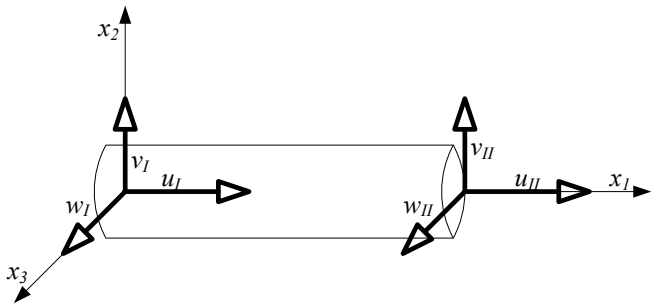

Figure 6.6 - Tri-dimensional finite element with three degrees freedom. Adpated from [18**].**

If a problem is discretized with *n* of nodes, so the total number of degrees of freedom is the product of *n* by the number of degrees of freedom for node. With the increasing of the total number of degrees of freedom of the system, more time is required for the calculus. Besides the displacement, the variables can be also nodal degrees of freedom of rotation.

Figure 6.7 - Example of a beam element with a rotation degree of freedom. Adapted from [18**].**

When the displacements are calculated, the numeric simulation software calculates the respective deformation and its stresses. Then the information is shown to the programmer in order to be analysed.

6.2.1. Methodology of resolution using the FEM

On a generally approach the tasks that a programmer do when is doing a simulation programme by the FEM are insert in three different stages:

- Pre-processing (i);
- Analysis (ii);
- Post-processing (iii).

6.2.1.1. Pre-processing

The pre-processing phase represents the construction of a geometric model of a system, including the loads and conditions of the problem. In commercial software this phase includes graphic tools that allow the user, to build easily the model of system to analyze. On this phase the user defines the parameters, namely the type of finite element, the mesh, mechanical properties, loads (forces, moments, pressure, etc), boundary conditions (constraints), so the global quality of the analysis is directly affected by the accuracy of the inputs.

This information is the input data to the system. In order to reduce the calculation time and the information generated, the user defines the set of results needed. When completed, the files of input data are submitted to the analysis phase.

6.2.1.2. Analysis

The analysis is the phase of process of numeric simulation by the FEM that the calculus is done. The phase begins with the verification of the information input on the file data, created by the user, and if no errors be detected the numeric simulation is done, being created output files with all information that user required.

6.2.1.3. Post-processing

The post-processor is the module that outputs the information of the result output files, through graphic tools or schedules, and the information displayed should be user-friendly. For

example the graphic tools can be coloured distributions of isovalues or isocolours. The post-processor can be included with the others items of the programme, in order to do the use of the programme easily and uniform. The different phases of a typical analysis of finite elements, on the point of view of user, can be summarized and systemized on Figure 6.8.

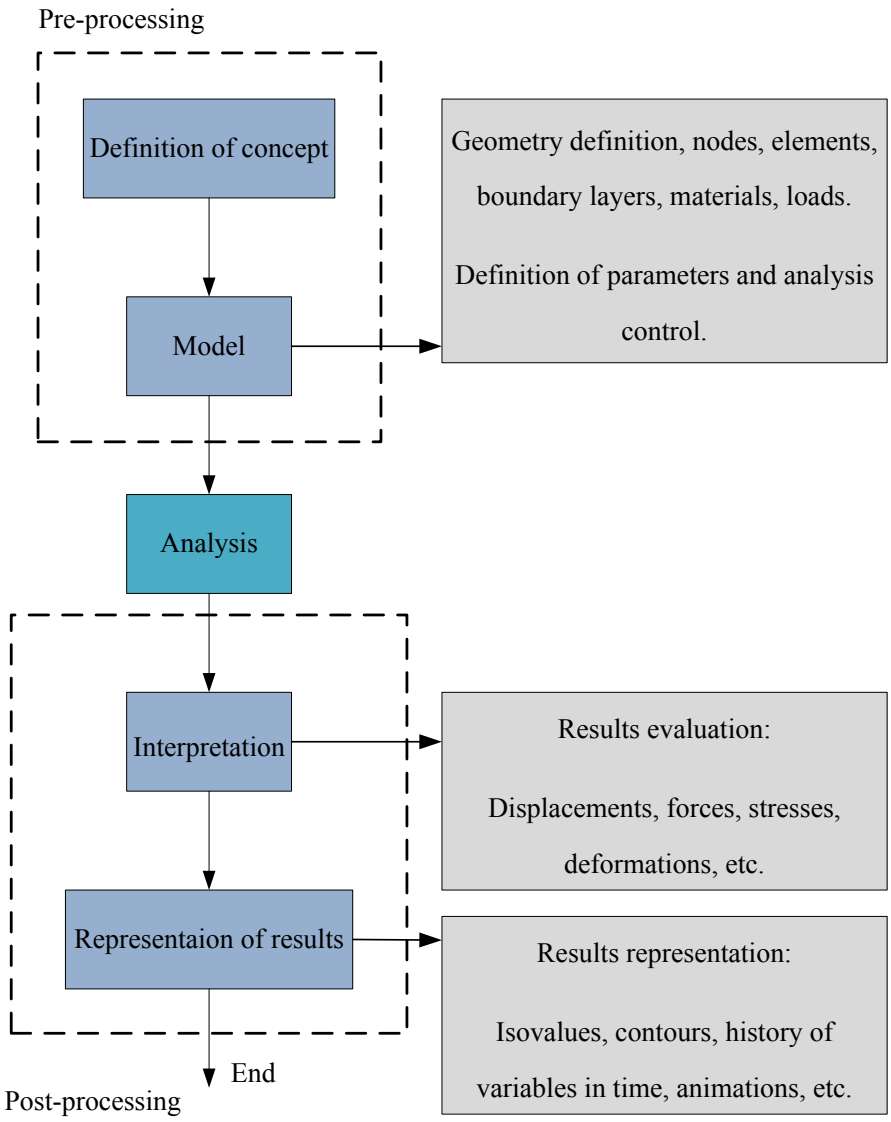

Figure 6.8 – Schematic representation of methodology of finite element analysis. Adapted from [19].

6.2.2. FEM on cable structures

In order to study the cable, a finite element the procedure developed elsewhere [**17**] is used. Further details can be obtained there.

6.2.2.1. Discretization of the finite element mesh

The element to use in this study is of cable type. It has two nodes on ends and three orthogonal independent displacements, where are a continuous series of elements connected by labelled link, submitted to nodal forces and large displacements.

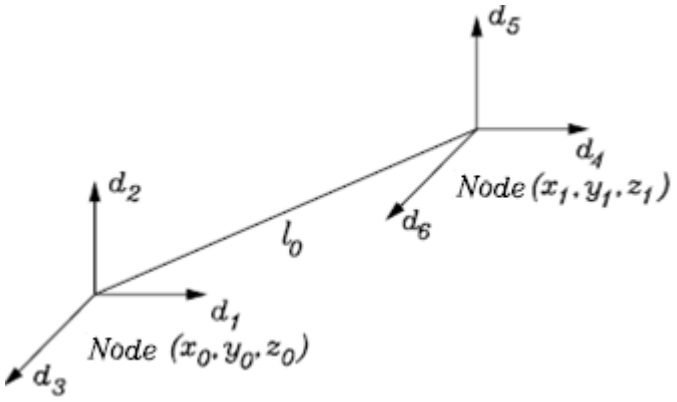

Figure 6.9 - Finite basic element. Adapted from [17].

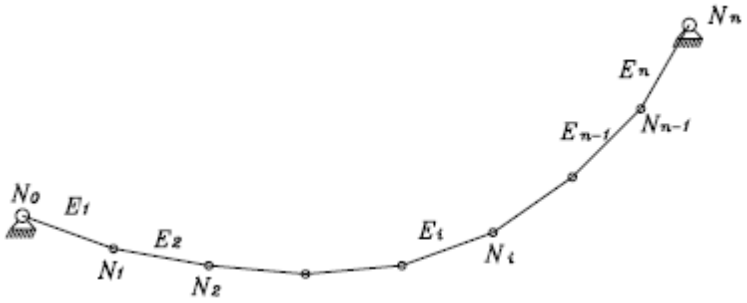

Figure 6.10 - Discretization of cable (n+1 nodes and n elements). Retrieved from [17].

The initial length, before the deformation, defines the initial configuration, which is calculated with the nodal coordinates. The initial length is given by (6.5).

$$l_0 = \sqrt{(x_1 - x_0)^2 + (y_1 - y_0)^2 + (z_1 - z_0)^2} \tag{6.5}$$

The vector of nodal displacements associated to the element, $\{d_1, d_2, d_3, d_4, d_5, d_6\}$, is defined by the three independent displacements of the two end nodes defining the element. This vector and the initial configuration will define the deformed configuration and the deformed length (6.6).

$$l = \sqrt{(x_1 + d_1 - x_0 - d_4)^2 + (y_1 + d_2 - y_0 - d_5)^2 + (z_1 + d_3 - z_0 - d_6)^2} \tag{6.6}$$

The direction of the displacement of each element is calculated by (6.7), (6.8) and (6.9).

$$\cos(\alpha_1) = \frac{x_1+d_1-x_0-d_4}{l} = \frac{l_x}{l} \tag{6.7}$$

$$\cos(\alpha_2) = \frac{y_1+d_2-y_0-d_5}{l} = \frac{l_y}{l} \tag{6.8}$$

$$\cos(\alpha_3) = \frac{z_1+d_3-z_0-d_6}{l} = \frac{l_z}{l} \tag{6.9}$$

6.2.2.2. Equilibrium conditions

The equilibrium on the three orthogonal directions, in which node of structure, is defined by equation (6.10).

$$K\Delta d = f_{ext} - f_{int} \tag{6.10}$$

The incremental vector is the unknown variable to be determinate. Due to the large displacements, the geometry is not constant, the stiffness coefficients and the internal forces depend on the geometry and therefore on the deformed configuration, [**17**].

The methodology of resolution of problem consists on an iterative strategy, and when the convergence is achieved, the deformed configuration and internal forces can be calculated.

6.2.2.2.1. Internal and external forces

Due to equilibrium the resultants of external forces and internal forces must be equal. The components of internal forces on a node are a function of the axial load acting on element, which depends from the deformed configuration (Figure 6.11), so the initial configuration and a vector of displacements are needed to obtain the internal forces. The six components of internal forces in the element are: ${f_{int}}^e = \{f_1, f_2, f_3, f_4, f_5, f_6,\}$, where, (6.11) :

$$\begin{cases} f_1 = F\cos(\alpha_1) = -f_4 \\ f_2 = F\cos(\alpha_1) = -f_5 \\ f_3 = F\cos(\alpha_1) = -f_6 \end{cases} \tag{6.11}$$

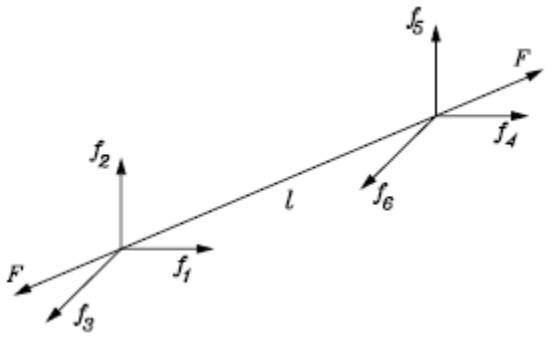

Figure 6.11 - Cartesian coordinates of internal forces. Retrieved from [17].

The global axial force F on the element is obtained by (6.12):

$$F = \Omega\sigma(\varepsilon) \tag{6.12}$$

The stress is a function of the field of displacements and is calculated by the constitutive law of material. The elastic linear (Hook's) law is given by (6.13).

$$\sigma = E\varepsilon \tag{6.13}$$

Taking into consideration that large displacements are considered, the Lagrangian formulation was used. The stiffness coefficients and internal forces where calculated with the definition of Lagrange-Green strain, (6.14).

$$\varepsilon = \frac{1}{2}\frac{l^2 - {l_0}^2}{{l_0}^2} \tag{6.14}$$

The external forces allocated on the nodes of extremity are defined by the vector: ${f_{ext}}^e = \{f_{i,1}, f_{i,2}, f_{i,3}, f_{i4}, f_{i5}, f_{i6},\}$.

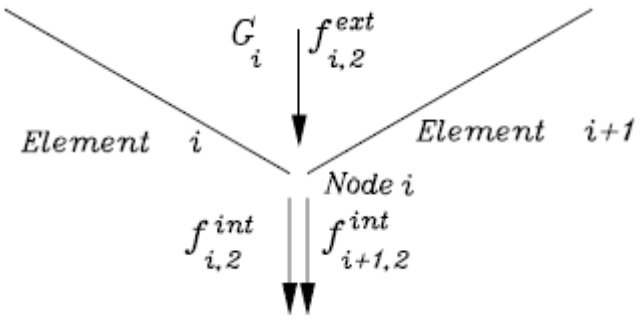

Figure 6.12 - Equilibrium of forces on node i. Adapted from [17].

The equilibrium conditions should be satisfied in each direction and for all nodes. The conditions of equilibrium for the three directions are given by (6.15), (6.16) and (6.17).

$$f_{ext} - f_{int} = {f_{i,2}}^{ext} - G_i - {f_{i,2}}^{int} + {f_{i+1,2}}^{int} = 0 \tag{6.15}$$

$$f_{ext} - f_{int} = {f_{i,1}}^{ext} - G_i - {f_{i,1}}^{int} + {f_{i+1,1}}^{int} = 0 \tag{6.16}$$

$$f_{ext} - f_{int} = {f_{i,3}}^{ext} - G_i - {f_{i,3}}^{int} + {f_{i+1,3}}^{int} = 0 \tag{6.17}$$

6.2.2.2.2. Stiffness matrix

The stiffness matrix coefficients of the cable element are not linear because the geometry is not constant; so the tangent matrix stiffness $f_i = F\cos(\alpha_i) = \sigma(\varepsilon)\Omega\cos(\alpha_i)$ characterizes the stiffness. The global tangent stiffness at cable, K, has a dimension $3(n-1) \times 3(n-1)$ and is obtained by the assembly of the tangent stiffness of each element, K^e, (a matrix with dimension 6×6), obtained by (6.18).

$$K^e = \begin{bmatrix} k & -k \\ -k & k \end{bmatrix} \tag{6.18}$$

k - Sub-matrix (3×3) is given by

$$k = \begin{bmatrix} k_{11} & k_{12} & k_{13} \\ k_{21} & k_{22} & k_{23} \\ k_{31} & k_{32} & k_{33} \end{bmatrix} \tag{6.19}$$

Knowing that:

$$f_i = F\cos(\alpha_i) = \sigma(\varepsilon)\Omega\cos(\alpha_i) \tag{6.20}$$

The matrix elements can be obtained by (6.21) and (6.22).

$$k_{i,j} = \frac{\partial_{f_i}}{\partial_{d_j}} = \Omega\frac{\partial_\sigma}{\partial_\varepsilon}\frac{\partial_\varepsilon}{\partial_{d_j}}\cos(\alpha_i) + F\frac{\partial_{\cos(\alpha_i)}}{\partial_{d_j}} \; if \; i = j \tag{6.21}$$

$$\begin{cases} k_{i,j} = \Omega \frac{\partial_\sigma}{\partial_\varepsilon} \frac{l_i l_j}{{l_0}^2 l} + F \frac{l^2 - {l_i}^2}{l^3} \ if \ i = j \\ k_{i,j} = \Omega \frac{\partial_\sigma}{\partial_\varepsilon} \frac{l_i l_j}{{l_0}^2 l} + F \frac{l_i l_j}{l^3} \ if \ \ i \neq j \end{cases} \tag{6.22}$$

where $i, j = 1,2,3$.

Therefore the six coefficients of tangent stiffness matrix are obtained by equation (6.23) to (6.28):

$$k_{11} = \Omega \frac{\partial_\sigma}{\partial_\varepsilon} \frac{l_x}{{l_0}^2} \frac{l_x}{l} + F \frac{l^2 - {l_x}^2}{l^3} \tag{6.23}$$

$$k_{22} = \Omega \frac{\partial_\sigma}{\partial_\varepsilon} \frac{l_y}{{l_0}^2} \frac{l_y}{l} + F \frac{l^2 - {l_y}^2}{l^3} \tag{6.24}$$

$$k_{33} = \Omega \frac{\partial_\sigma}{\partial_\varepsilon} \frac{l_z}{{l_0}^2} \frac{l_z}{l} + F \frac{l^2 - {l_z}^2}{l^3} \tag{6.25}$$

$$k_{12} = \Omega \frac{\partial_\sigma}{\partial_\varepsilon} \frac{l_x}{{l_0}^2} \frac{l_y}{l} + F \frac{l_x l_y}{l^3} \tag{6.26}$$

$$k_{13} = \Omega \frac{\partial_\sigma}{\partial_\varepsilon} \frac{l_x}{{l_0}^2} \frac{l_z}{l} + F \frac{l_x l_z}{l^3} \tag{6.27}$$

$$k_{23} = \Omega \frac{\partial_\sigma}{\partial_\varepsilon} \frac{l_y}{{l_0}^2} \frac{l_z}{l} + F \frac{l_y l_z}{l^3} \tag{6.28}$$

where:

$$\frac{\partial_\sigma}{\partial_\varepsilon} = E, l_x = l_1, l_y = l_2, l_z = l_3 \tag{6.29}$$

$$\frac{\partial_{\cos(\alpha_1)}}{\partial_{d_i}} = \left[\frac{l^2 - {l_x}^2}{l^3}, -\frac{l_x l_y}{l^3}, -\frac{l_x l_z}{l^3} \right], i = 1,2,3 \tag{6.30}$$

$$\frac{\partial_{\cos(\alpha_2)}}{\partial_{d_i}} = \left[-\frac{l_y l_x}{l^3}, -\frac{l^2 - {l_y}^2}{l^3}, -\frac{l_y l_z}{l^3} \right], i = 1,2,3 \tag{6.31}$$

$$\frac{\partial_{\cos(\alpha_i)}}{\partial_{d_i}} = \left[-\frac{l_x l_z}{l^3}, -\frac{l_y l_z}{l^3}, -\frac{l^2 - {l_z}^2}{l^3}\right], i = 1,2,3 \tag{6.32}$$

$$\frac{\partial_\varepsilon}{\partial_j} = \frac{l_j}{{l_0}^2}, j = 1,2,3 \tag{6.33}$$

6.2.3. Newton-Raphson method

In order to resolve (6.10), an iterative process based on the Newton-Raphson method is implemented. The calculation begins with the input the initial values of stiffness and internal forces; so initial values of the vector of displacements must be given; in this way an initial geometry and deformed geometry must be defined.

Assuming the equilibrium and linear behaviour, the equation (6.34) is valid in all nodes.

$$K_i \Delta d_i = f_{ext,i} - f_{int,i} \tag{6.34}$$

This equation is resolved and the vector increment of displacement Δd_i is calculated and a new vector of total displacements is obtained by: (6.35).

$$d_{i+1} = d_i + \Delta d_i \tag{6.35}$$

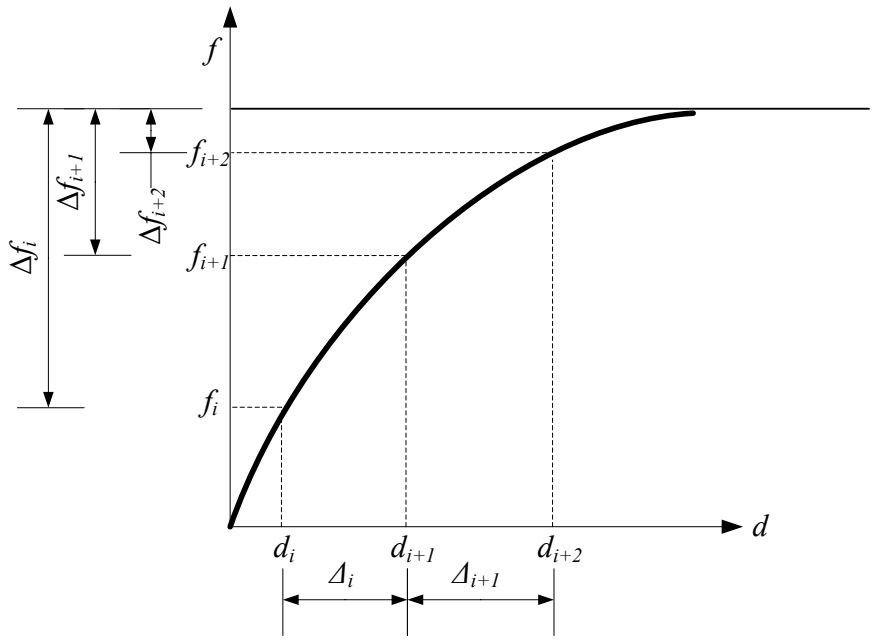

Figure 6.13 - Newton-Raphson method Adapted from [17].

This new vector of displacements and the constant vector of initial geometry together define the deformed configuration on the next step.

For an iterative process, in particular to the Newton-Raphson, the better the initial estimation of the vector of displacements, more quickly will converge to final solution. The incremental

process ends when the vector of internal forces is close enough of the vector of external forces, (6.36).

$$f_{ext,i} - f_{int,i} \leq Error \tag{6.36}$$

Or when the increment vector of displacement of iteration i +1 is sufficiently close to the vector obtained in iteration i, (6.37).

$$\left|\frac{d_{i+1}}{d_i} - 1\right| \leq Error \tag{6.37}$$

6.2.3.1. Computational implementation

The computational implementation is based on the numeric description, based on the finite element analysis. The calculus begins with an initial configuration, a vector of initial node displacements and parameters in order to calculate an increment vector of displacements. The initial deformation and a new vector of displacements define the deformed configuration in the next iteration. The process can be described as follows:

- The initial configuration for the cable, allows the determination of the initial position of nodes;
- A vector of initial deformations is defined, considering a geometry slightly different;
- The initial tangent stiffness and initial internal forces are calculated by (6.11) (6.21) and (6.22);
- The total equilibrium conditions (6.10) are imposed and Δd is calculate;
- A new vector of displacements is calculated using (6.35);
- The step 2 is repeated until the convergence is achieved.

6.3. Programme evaluation

To use the FEM applications on cable, a programme based on the Lagrangean formulation and Newton-Raphson method are developed, in order to obtain a solution by finite element on a two-dimensional cable (the programme also allows the study of a three-dimensional cable). On Annex 1 is presented the list of programme developed.

To evaluate the performance of the programme, two solutions were compared. One using a standard example calculated with catenary equation and the other one using the "ANSYS R11 Academic Edition" software.

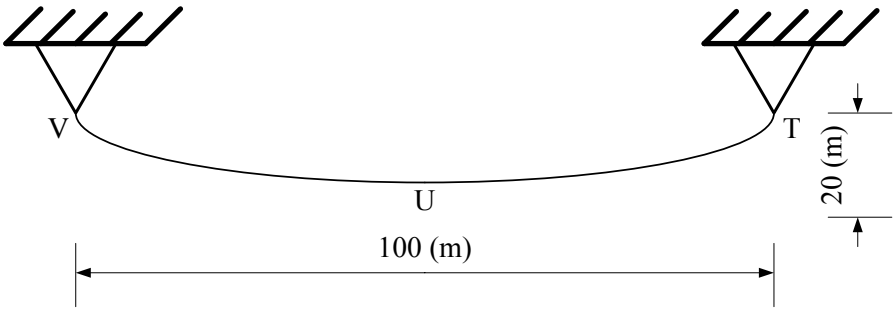

Figure 6.14 – Illustration of a cable with two fixed ends.

Without deformation the cable has the characteristics exposed on Table 6.1.

Table 6.1 - Characteristics of cable.

Material	ρ_{steel} **(kg/m^3)**	E_{steel} **(GPa)**	ν	r_{cable} **(m) [10^{-3}]**	Ω **(m^2) [10^{-4}]**	l_2 **(m)**	g **(m/s^2)**	$W_{cat\ cable}$ **(N/m)**
Steel (S235)	7850, [**11**]	210, [**11**]	0.3	15	7.069	109.975	9.810	54.437

The analysis took into account:

- Analytical solution;
- Bi fixed system;
- One extremity fixed and other cantilever with the correspondent reaction.

6.3.1. Analytical solution

The analytical equation of catenary follows the procedure presented on [**20**]. The origin of coordinate system, 0, is allocated below the lowest point of the catenary, U, to a distance c.

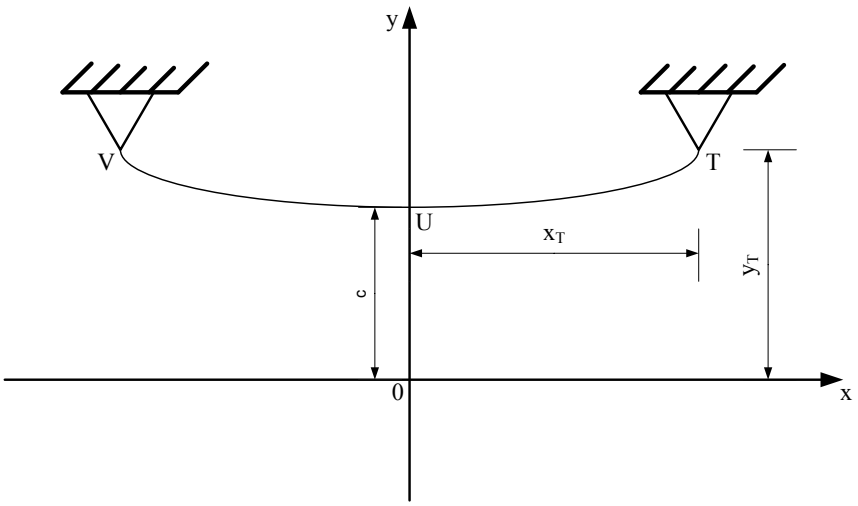

Figure 6.15 - Illustration of the coordinates of point T.

The coordinates of the point T are:

$$x_T = 50\ (m)$$

$$y_T = 20 + c\ (m)$$

If these values were substituted on the equation (6.1), it is obtained:

$$20 + c = c\cosh\left(\frac{50}{c}\right)$$

The value of c is determined by iteration and its value is, c= 65.590, with an approximation error of 0.1 % which is acceptable. The coordinates of deformed geometry are:

Table 6.2 - Coordinates of deformed geometry.

x (m)	y (m)	F (N)
-50	85.590	4659.289
-40	78.170	4255.349
-30	72.571	3950.583
-20	68.663	3737.826
-10	66.354	3612.122
0	65.590	3570.543
10	66.354	3612.122
20	68.663	3737.826
30	72.571	3950.583
40	78.170	4255.349
50	85.590	4659.289

The maximum stress on cable is obtained by (6.38).

$$\sigma_{max} = \frac{F_{max}}{\Omega} \tag{6.38}$$

For this particular case the length of cable, l, is determinate by (6.39).

$$l = 2 \times \sqrt{{y_t}^2 - c^2} \tag{6.39}$$

The values of minimum and maximum tension on cable (obtained by (6.3) and (6.4)), maximum stress and cable length are presented on Table 6.3.

Table 6.3 - Values of tension, stress and length obtained by the model of catenary.

F_{min} (N)	F_{max} (N)	σ_{max} (MPa)	l_2 (m)
3570.543	4659.289	6.059	109,975

6.3.2. Programme's solution

The programme has two versions, one refers to a cable with two fixed ends supporting its self weight (A version) and in the other one, an end was released and the respective reaction was allocated on referent node (B version). On Annex 2 and Annex 3 are presented the list of input files of programme's A and B version respectively.

6.3.2.1. Programme's A version

The initial geometry proposed is based on the catenary solution. A difference is the position of the reference, comparably to analytical solution, which is allocated on the left end.

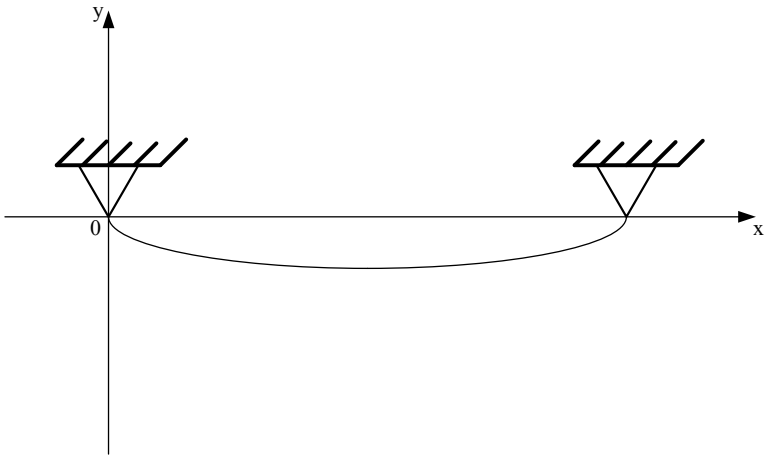

Figure 6.16 - Illustration of the initial configuration proposed and position of the reference of coordinates of cable on programme.

The coordinates of points for the programme are given by (6.40) and (6.41).

$$x_P = x - x_T \tag{6.40}$$

$$y_P = -y_T + y \tag{6.41}$$

The coordinates of nodes of the initial geometry are presented on Table 6.4.

Table 6.4 - Coordinates of nodes of the initial geometry.

x (m)	y (m)	x_P (m)	y_P (m)
-50	85.590	0	0.000
-40	78.170	10	-7.419
-30	72.571	20	-13.018
-20	68.663	30	-16.926
-10	66.354	40	-19.235
0	65.590	50	-19.999
10	66.354	60	-19.235
20	68.663	70	-16.926
30	72.571	80	-13.018
40	78.170	90	-7.419
50	85.590	100	0.000

The incremental weight of elements is obtained by (6.42):

$$W_{element} = \frac{W_{catcable} \times l_2}{n_{elements}} \tag{6.42}$$

The number of elements chosen was 10, and takes in account the values of $W_{catcable}$ and l_2, the weight of elements is:

$$W_{element} = 598.672\ (N)$$

At the end of 38 iterations, with an error of 2.252 x 10^{-16}, the deformed geometry is presented on Figure 6.17.

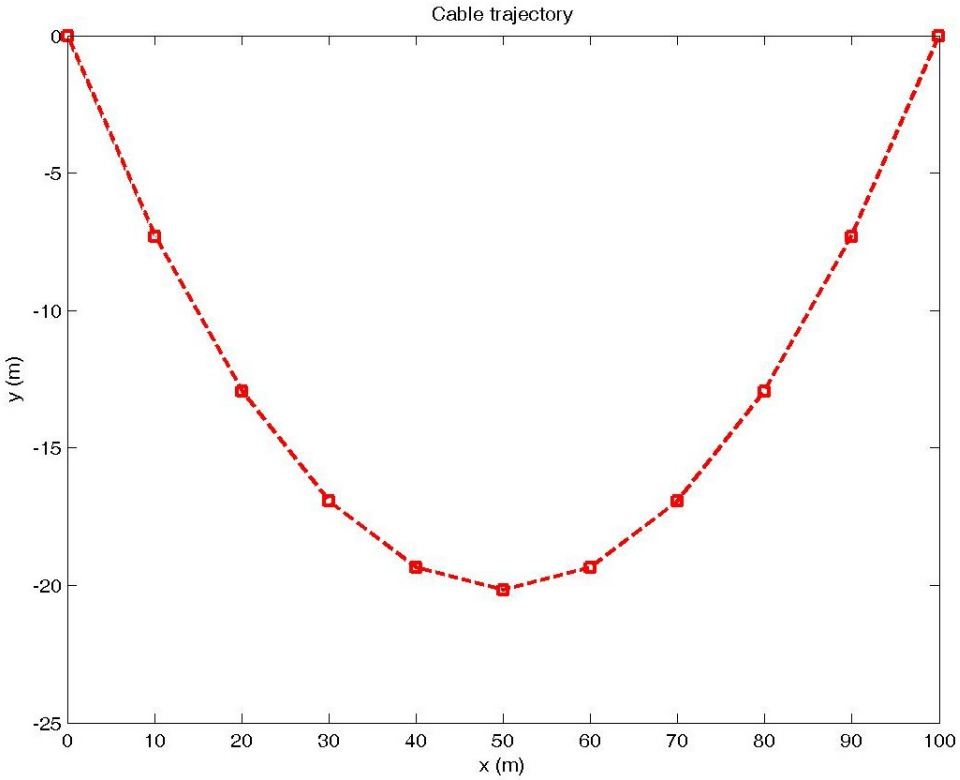

Figure 6.17 - Illustration of the deformed geometry for programme's A version.

The displacements on nodes and the global coordinates of deformed nodes for programme's A version, are presented on Table 6.5.

Table 6.5 - Displacements on nodes and global coordinates of deformed nodes for programme's A version.

Node	Δ_x (m)	Δ_y (m)	x (m)	y (m)
1	3.670E-10	-2.365E-11	-50	85.590
2	8.256E-02	1.119E-01	-39.917	78.282
3	6.674E-02	8.311E-02	-29.933	72.654
4	2.656E-02	-1.896E-02	-19.973	68.644
5	2.965E-03	-1.200E-01	-9.997	66.234
6	-2.700E-15	-1.610E-01	0	65.429
7	-2.965E-03	-1.200E-01	9.997	66.234
8	-2.656E-02	-1.896E-02	19.973	68.644
9	-6.674E-02	8.311E-02	29.933	72.654
10	-8.256E-02	1.119E-01	39.917	78.282
11	-3.670E-10	-2.365E-11	50	85.590

The internal forces on the elements for programme's A version are presented on Table 6.6.

Table 6.6 -Internal forces on the elements for programme's A version.

Element	F_x (N)	F_y (N)	F (N)
1	3717.300	-2694.000	4590.900
2	3717.300	-2095.300	4267.200
3	3717.300	-1496.700	4007.300
4	3717.300	-898.010	3824.200
5	3717.300	-299.340	3729.300
6	3717.300	299.340	3729.300
7	3717.300	898.010	3824.200
8	3717.300	1496.700	4007.300
9	3717.300	2095.300	4267.200
10	3717.300	2694.000	4590.900

6.3.2.2. Programme's B version

On programme's B version takes the same features of programme's A version, but the right end is released and the reaction on element 10 (from programme's A version) is inputted on the node 11. So a value of F_x 3717.3 (N), F_y 2694 (N) are inputted. At the end of 35 iterations, with an error of 1.233×10^{-13}, the deformed geometry is presented on Figure 6.18.

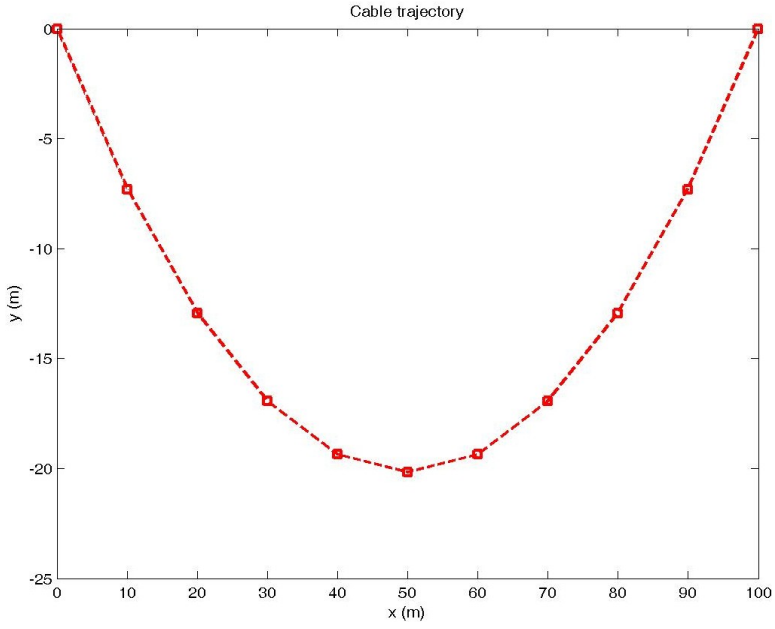

Figure 6.18 - Illustration of the deformed geometry for programme's B version.

The displacements on nodes and the global coordinates of deformed nodes for programme's B version, are presented on Table 6.7

Table 6.7 - Displacements on nodes for programme's B version.

Node	Δ_x (m)	Δ_y (m)	x (m)	y (m)
1	1.203E-12	-1.109E-11	-50.000	85.590
2	8.225E-02	1.115E-01	-39.918	78.282
3	6.621E-02	8.229E-02	-29.934	72.653
4	2.590E-02	-2.011E-02	-19.974	68.643
5	2.243E-03	-1.214E-01	-9.998	66.233
6	-7.314E-04	-1.625E-01	-0.001	65.428
7	-3.698E-03	-1.215E-01	9.996	66.233
8	-2.733E-02	-2.031E-02	19.973	68.643
9	-6.760E-02	8.200E-02	29.932	72.653
10	-8.359E-02	1.111E-01	39.916	78.281
11	-1.299E-03	-4.419E-04	49.999	85.590

The internal forces on the elements for programme's B version, are presented on Table 6.8

Table 6.8 - Internal forces on the elements for programme's B version.

Element	F_x (N)	F_y (N)	F (N)
1	3717.000	-2694.000	4590.600
2	3717.000	-2095.400	4266.900
3	3717.000	-1496.700	4007.000
4	3717.000	-898.030	3823.900
5	3717.000	-299.350	3729.000
6	3717.000	299.320	3729.000
7	3717.000	897.990	3823.900
8	3717.000	1496.700	4007.000
9	3717.000	2095.300	4266.900
10	3717.600	2694.400	4591.300

6.3.3. Software solution

The coordinates of nodes of the initial geometry for the software are the same of Table 6.4, the constants inputted are the g, E_{steel}, r_{cable} present on Table 6.1. The non linear analysis for large displacements is used. The displacements on nodes and the global coordinates of deformed nodes for software are presented on Table 6.9.

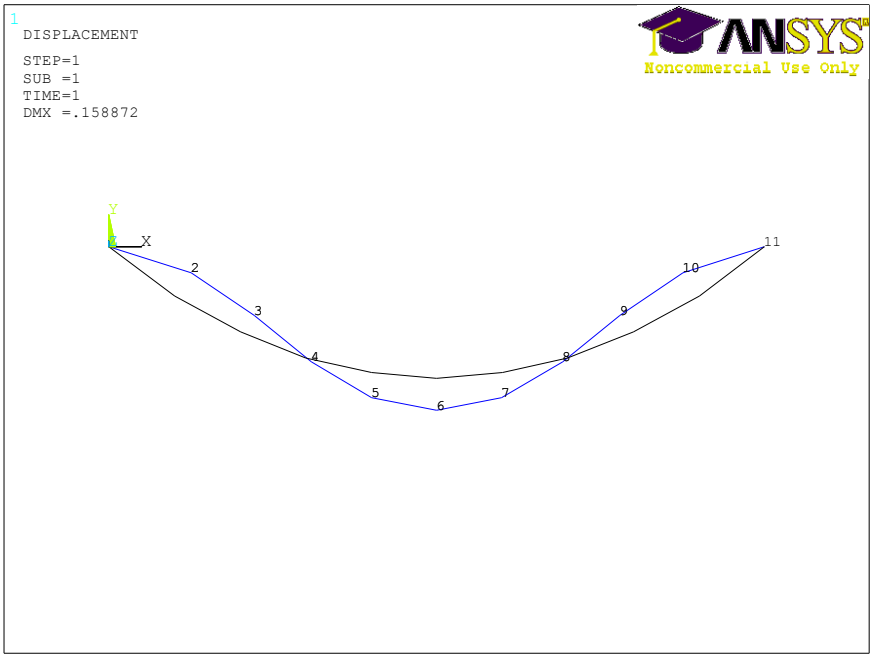

Figure 6.19 - Illustration of the deformed geometry according to ANSYS software.

Table 6.9 - Displacements on nodes for software.

Node	Δ_x (m)	Δ_y (m)	x (m)	y (m)
1	0	0	-50.000	85.590
2	0.080	0.109	-39.920	78.279
3	0.066	0.083	-29.934	72.654
4	0.026	-0.019	-19.974	68.644
5	0.003	-0.118	-9.997	66.236
6	-1.452E-12	-0.159	0	65.431
7	-0.003	-0.118	9.997	66.236
8	-0.026	-0.019	19.974	68.644
9	-0.066	0.083	29.934	72.654
10	-0.080	0.109	39.920	78.279
11	0	0	50.000	85.590

The internal forces on the elements for software are presented on Table 6.10.

Table 6.10 - Internal forces on the elements for software.

Element	F_x (N)	F_y (N)	F (N)
1	3718.000	-2694.500	4591.716
2	3717.400	-2095.500	4267.339
3	3718.000	-1497.000	4008.059
4	3717.400	-898.060	3824.340
5	3717.300	-299.340	3729.333
6	3717.300	299.340	3729.333
7	3717.400	898.060	3824.340
8	3718.000	1497.000	4008.059
9	3717.400	2095.500	4267.339
10	3718.000	2694.500	4591.716

6.3.4. Analysis of results

On this topic the results are analysed from the point of view of the difference between the results and the value that are expectable to obtain. The value that is considerate more reliable is the value obtained by the commercial software of finite element because is software that is dedicated to structure analysis and have internal algorithms which can have into account coefficients adapted to reality.

The relative error between the results from programmes or analytical equation with software results, take into account the displacements and forces, are given by (6.43).

$$Re\ (\%) = \left|\frac{R_a - R_s}{r_s}\right| \times 100 \tag{6.43}$$

6.3.4.1. Deformed geometry

The initial deformed configuration proposed for programmes and for software was the configuration of catenary and the relative error between the software/analytical equation and software/programmes for the displacements is small, so the initial geometry is close from the final one.

Table 6.11 – Comparison of deformed geometry between the analytical equation and software.

	Analytical equation		Software		Re_x (%)	Re_y (%)
Node	x (m)	y (m)	x (m)	y (m)		
1	-50	85.590	-50.000	85.590	0	0.000
2	-40	78.170	-39.920	78.279	0.200	0.139
3	-30	72.571	-29.934	72.654	0.220	0.114
4	-20	68.663	-19.974	68.644	0.130	0.028
5	-10	66.354	-9.997	66.236	0.030	0.178
6	0	65.590	0	65.431	0	0.243
7	10	66.354	9.997	66.236	0.030	0.178
8	20	68.663	19.974	68.644	0.130	0.028
9	30	72.571	29.934	72.654	0.220	0.114
10	40	78.170	39.920	78.279	0.200	0.139
11	50	85.590	50.000	85.590	0	0.000

The value of relative error shown on Table 6.11, is less than 0.25 % showing that the model of catenary and the software of finite element produce nearly the same results of displacements. The law level of tension, do that the results of FEM are less influenced by the geometric nonlinearity, [**17**].

The relative error for the displacements between programme's A version and the software is presented on Table 6.12.

Table 6.12 - Relative error for displacements between programme's A version and software.

Node	Programme's A version		Software		Re_x (%)	Re_y (%)
	x (m)	y (m)	x (m)	y (m)		
1	-50	85.590	-50	85.590	0	0
2	-39.917	78.282	-39.920	78.279	0.008	0.004
3	-29.933	72.654	-29.934	72.654	0.003	0
4	-19.973	68.644	-19.974	68.644	0.005	0
5	-9.997	66.234	-9.997	66.236	0	0.003
6	0	65.429	0	65.431	0	0.003
7	9.997	66.234	9.997	66.236	0	0.003
8	19.973	68.644	19.974	68.644	0.005	0
9	29.933	72.654	29.934	72.654	0.003	0
10	39.917	78.282	39.92	78.279	0.008	0.004
11	50	85.590	50	85.590	0	0

The value of relative error shown on Table 6.12 is nearly 0 % showing that the programme's A version and the software of finite element produce nearly the same results of displacements.

The relative error for the displacements between programme's B version and the software is presented on Table 6.13.

Table 6.13 - Relative error for displacements between programme's B version and software.

Node	Programme's B version		Software		Re_x (%)	Re_y (%)
	x (m)	y (m)	x (m)	y (m)		
1	-50	85.590	-50	85.590	0	0
2	-39.918	78.282	-39.92	78.279	0.005	0.004
3	-29.934	72.653	-29.934	72.654	0	0.001
4	-19.974	68.643	-19.974	68.644	0	0.001
5	-9.998	66.233	-9.997	66.236	0.010	0.005
6	-0.001	65.428	0	65.431	0	0.005
7	9.996	66.233	9.997	66.236	0.010	0.005
8	19.973	68.643	19.974	68.644	0.005	0.001
9	29.932	72.653	29.934	72.654	0.007	0.001
10	39.916	78.281	39.92	78.279	0.010	0.003
11	49.999	85.590	50	85.590	0.002	0.000

The results of programme's B version are almost the same of programme's A version, which demonstrates that the programme's B version keeps the key characteristics of programme relatively to displacements.

6.3.4.2. Internal forces

The relative error for the internal forces between the analytical equation and the software results is presented on Table 6.14.

Table 6.14 . Relative error for internal forces between analytical equation and software.

Analytical equation		Software		Re_{min} (%)	Re_{max} (%)
F_{min} (N)	F_{max} (N)	F_{min} (N)	F_{max} (N)		
3570.543	4659.289	3729.233	4591.716	4.258	1.472

The relative error for the internal forces between the analytical equation and the software results is 4.258 % for the minimum force and 1.472 % for the maximum force. It would expect that the relative error was smaller because the cross section area is large enough to obtain a small value of stress and finite element analysis is little affected by the low level of stress, [**17**]. Perhaps the determination of the weight of cable can induce errors. However for situations where large deformations occur, the change in geometry changes the deformed and the FEM can be more realistic, [**17**].

The relative error between internal forces between programme's A version and programme's B version with software are shown on Table 6.15 and Table 6.16 respectively.

Table 6.15 - Relative error for internal forces between programme's A version and software.

Programme's A version		**Software**		Re_{min} (%)	Re_{max} (%)
F_{min} (N)	F_{max} (N)	F_{min} (N)	F_{max} (N)		
3729.300	4590.900	3729.233	4591.716	0.001	0.018

Table 6.16 - Relative error for internal forces between programme's B version and software.

Programme's B version		**Software**		Re_{min} (%)	Re_{max} (%)
F_{min} (N)	F_{max} (N)	F_{min} (N)	F_{max} (N)		
3729.000	4590.6	3729.233	4591.716	0.009	0.024

The result of the programme's A version and the software have a relative error of 0.018% for the maximal force and 0.001% for the minimal force. The results of the programme's B version and the software have a relative error of 0.024% for the maximal force and 0.009% for the minimal force. Considering that the relative error between programmes and the software is nearly 0%, is possible to conclude that the programmes developed are coherent with the numerical analysis provided by the software confirms that it is adequate to resolve structural analysis of cables.

The results of programme's B version are almost the same of programme's A version, which demonstrates that the programme's B version keeps the key characteristics of programme's A

version and for the specific case of the lift force that is variable, the programme's B version has the advantage of the one end can be removed which allows the input of a variable lift force. The solution obtained by the analytical equation assumes a rigid geometrical configuration, in other words, the deformation is formulated assuming that the cable is inextensible. The stress distribution and geometry of cable follow that function. The referred to equations are valid only for elastic domain, with small deformations, to approximate the model condition of inextensible cable.

The catenary model cannot be implemented to the present case, because there are horizontal distributed forces, produced by the wind and in order to achieve equilibrium it is necessary to have horizontal forces at fixed ends, which do not exist on the catenary model.

Perhaps a model of catenary with modifications, that takes into account the increase in length, and neglecting wind forces on cable could be envisaged. However, the variable height continuing changing, as well as the variable drag on the aero module, results very complex to implement. If we consider drag on cable the model is no longer valid. For situations where large deformations occur, the geometry isn't constant, so the internal strains depended from the geometry and are function of configuration of deformed, [**17**].

6.4. Structural analysis of cable

The purpose of this topic is to show an example of the influence that the developed programme can have on the control of the system. The goal is to adjust the lift force in order to set the value of force at the lower end (element 1) nearly constant. Taking into account that rigorous results for the aerodynamics forces are unknown, the values of forces in a bi dimensional situation are given as example, which take into consideration the maximum force that cable can support and energy specifications provided. For the solution, the following data must be input:

- Initial geometry - the corresponded nodes and elements. The number of iterations will be lower if the initial geometry be closer from the deformed geometry;
- Sections properties - Variables as the cross section area and Young modules of material;
- Loads - Cable weight which is applied ate the nodes of cable, lift force (force of unwinding) and the drag forces on cable.

6.4.1. Initial geometry

The initial geometry proposed is a parabola, considering that the cable will be nearly as parabolic geometry. The parabola equation is given by (6.44).

$$f(x) = x^2 \tag{6.44}$$

The length of cable l_3 is determined by (6.45).

$$l_3 = \int_a^b \sqrt{1 + (f'(x))^2} \tag{6.45}$$

In this is obtained (6.46).

$$l_3 = \int_a^b \sqrt{1 + (2x)^2} \tag{6.46}$$

Considering a range between 0 and x, the length of parabola is given by (6.47).

$$l_3 = \frac{\sinh(2x)}{4} + x\sqrt{x^2 + \frac{1}{4}} \tag{6.47}$$

6.4.2. Section properties

The material to implement is a UHMPE; has a low Young modulus leading to large elastic displacements. The properties are presented on Table 6.17.

Table 6.17 - Section properties of cable.

E_{UHMPE} (GPa)	Ω (m^2) [10^{-4}]
0.483	1.539

6.4.3. Loads

As an example if we consider the unwinding cycle, after the transient regime, considering that 15 seconds passed since the initial moment, at a speed of unwinding of 4 (m/s), the amount of cable unwound is about 210 (m). Taking into account the geometry of the parabola, a value of 225 (m) for y is chosen, corresponding to a cable length of 226.149 (m). The weight of cable for unit of length is 5.963 (N/m), the force of unwinding is 30000 (N) with a $\measuredangle$ 60º orientation, and due to the fact that wind velocity changes with height there is a gradient in the horizontal forces, which varies in the range of 10 to 1000 (N).

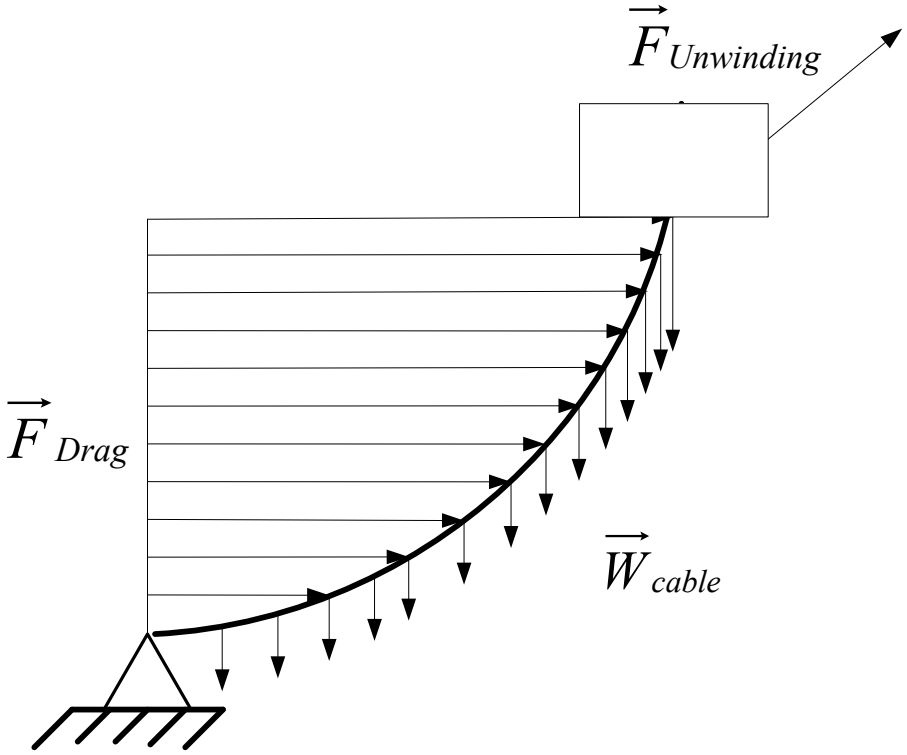

Figure 6.20 – Schematically diagram of external forces applied on structure.

The coordinates, incremental length of cable and forces on nodes are presented on Table 6.18. The description of elements and corresponding nodes are presented on Table 6.19.

Table 6.18 - Coordinates of nodes incremental length of cable and forces on nodes.

Node	x (m)	y (m)	$l_3\ (m)$	F_x (N)	F_y (N)
1	0	0	0.000	10.000	0.000
2	1	1	1.479	76.000	8.819
3	2	4	4.647	142.000	18.890
4	3	9	9.747	208.000	30.413
5	4	16	16.819	274.000	42.168
6	5	25	25.874	340.000	53.999
7	6	36	36.920	406.000	65.864
8	7	49	49.958	472.000	77.748
9	8	64	64.992	538.000	89.644
10	9	81	82.021	604.000	101.546
11	10	100	101.047	670.000	113.454
12	11	121	122.071	736.000	125.365
13	12	144	145.093	802.000	137.279
14	13	169	170.113	868.000	149.194
15	14	196	197.131	934.000	161.111
16	15	225	226.149	16000.000	26153.792

Table 6.19 - Description of elements and corresponding nodes.

Nodes	Elements	Nodes	Elements
1 → 2	1	8 → 9	8
2 → 3	2	9 → 10	9
3 → 4	3	10 → 11	10
4 → 5	3	11 → 12	11
5 → 6	5	12 → 13	12
6 → 7	6	13 → 14	13
7 → 7	7	14 → 15	14
8 → 9	8	15 → 16	15

At the end of 1995 iterations, with an error of 8.162×10^{-10}, the deformed geometry is presented on Figure 6.21.

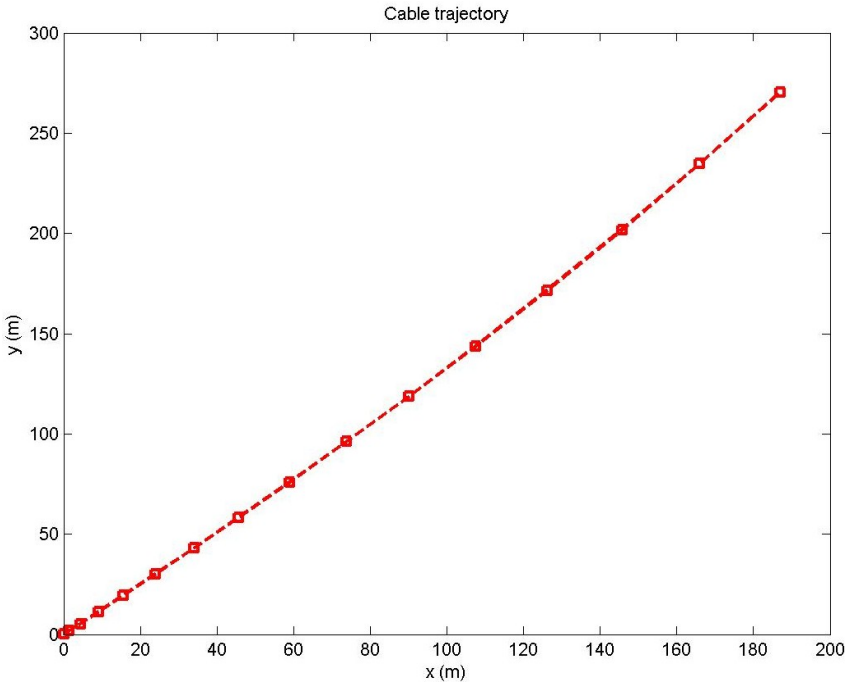

Figure 6.21 - Illustration of the deformed geometry.

The displacements on nodes and the global coordinates of deformed nodes for the example are presented on Table 6.20.

Table 6.20 - Value of displacements on nodes.

Node	Δ_x (m)	Δ_y (m)	Node	Δ_x (m)	Δ_y (m)
1	6.029E-08	6.744E-08	9	52.045	10.186
2	0.351	0.601	10	66.116	12.883
3	2.366	1.182	11	81.610	16.006
4	6.206	1.965	12	98.405	19.598
5	11.877	3.000	13	116.360	23.702
6	19.351	4.314	14	135.320	28.370
7	28.580	5.932	15	155.090	33.655
8	39.503	7.880	16	175.480	39.617

The internal forces on the elements are presented on Table 6.21.

Table 6.21 - Value of forces on elements.

Element	F_x (N)	F_y (N)	F (N)
1	23070	27329	35765
2	22994	27320	35709
3	22852	27302	35603
4	22644	27271	35447
5	22370	27229	35240
6	22030	27175	34983
7	21624	27109	34677
8	21152	27031	34324
9	20614	26942	33923
10	20010	26840	33478
11	19340	26727	32990
12	18604	26601	32461
13	17802	26464	31895
14	16934	26315	31293
15	16000	26154	30660

Is possible to note that the tension on element 1 is greater than 30 000 (N), so the lift value should lesser in order to keep as possible the value nearly constant on 30000 (N).

The intention of example is to show that the algorithm is capable to determine the tension on cable, in particular at the ends, and in this way to control the lift force. This control can be done if data be available of known and similar conditions. Tests should be done for different heights, cable lengths, meteorological conditions, orography and roughness of places in order to create a phenomenological analysis of the process.

7. Conclusions and future work

From this work several conclusions can be drawn:

- The prototype uses a lift force in order to produce work that is transformed into electric energy. This is a new and patented concept competing with other existing ones, like the traditional wind turbine and de MARS concept;
- The energy production cycle must be analyzed taking into account the transient regime that occurs during the transitions winding-unwinding, due to the inertia of the kinematic chain between the capstan and the motor/generator;
- A flywheel should be used to accumulate energy that can be used in the transient periods of the up-down cycle, being the energy to store 862.5 (kJ) and the inertia moment of 69.911 (kg m^2);
- The cable dimensioning done required some estimated data, namely the cross section area. This is due to the fact that the cable must be designed and manufactured and only after this one can have the actual data of the cable;
- The cable winding and unwinding must be done using a capstan in order to reduce the tension on the cable being wound on the storing drum;
- The results of the algorithm are consistent with the results of software of finite elements, demonstrating that it is adequate to resolve structural analysis of cables;
- In order to have credible data to develop the design and construction of the device, tests on prototype are required to get data for different heights, cable lengths, meteorological conditions, and characteristics of the implementation site.

Future work is necessary as to complement the information necessary:

- Control system development (hardware e software);
- Aerodynamic studies around the prototype;
- Development of a platform to hold the overall system to the ground;

- Breaking systems;
- Platform rotational system to provide the right orientation;
- Untwisting device for the cable.

References

[1] Tiago Pardal and Marco Freire, "ATMOSPHERIC RESOURCES EXPLORER," 20090278353, November 12, 2009.

[2] João Nuno Sousa, "Previsão da Produção Eléctrica em Parques Eólicos," Departamento de Engenharia Electrotécnica e de Computadores, Faculdade de Engenharia da Universidade do Porto, Porto, Master´s Thesis degree 2007.

[3] [Online]. http://sealevel.jpl.nasa.gov/overview/climate-climatic.html

[4] Henrik Kudsk, "Basic Wind Power Training," Vestas, 2008.

[5] Julia Layton. howstuffworks. [Online]. http://science.howstuffworks.com/wind-power3.htm

[6] "GLOBAL WIND 2009 REPORT," March 2010. [Online]. http://www.gwec.net/fileadmin/documents/Publications/Global_Wind_2007_report/GWEC_Global_Wind_2009_Report_LOWRES_15th.%20Apr.pdf

[7] "Global Wind Energy Outlook 2008," Global Wind Energy Council, 2008.

[8] "Indian Wind Energy Outlook 2009," Global Wind Energy Council, 2009.

[9] Magenn Power Inc. [Online]. http://www.magenn.com/products.php

[10] Lankhorst Ropes. [Online]. http://www.lankhorstropes.com/files/producten/9f81d9afc80a09d43f496f18d4392088.pdf

[11] Ferdinand P. Beer and E. Russel Johnston Jr., *Mecânica dos Materiais*, 3rd ed. Lisboa: McGRAW-HILL de Portugal, L., 2003.

[1 Fiber-Reinforced Grades, Rilsan® PA12. [Online]. 2] http://www.arkema.com/sites/group/en/products/detailed_sheets/technical_polymers/rilsan_12/product_info/key_properties_english_units.page

[1 Luciano de Oliveira Faria, *ÓRGÃOS DE MÁQUINAS 2ª PARTE*. Lisbon: AEIST, 1959, 3] vol. I.

[1 Wen-ji ZENG and Ai-jun CHEN, "WEIGHT FUNCTION FOR STRESS INTENSITY 4] FACTORS IN," ISSN 0253-4827, 2006.

[1 E.J. Hearn, *Mechanics of Materials 2*. Hong Kong: Elsevier Ltd, 1997.
5]

[1 J. P. Den Hartog, *ADVANCED STRENGTH OF MATERIALS*. United States of America: 6] McGraw-Hill Book Company, Inc., 1952.

[1 Humberto Varum and Rui Cardoso, Geometrical non-linear model for the analysis of cable 7] structures.

[1 João Burguete Cardoso, "Introdução ao M.E.F.," DEMI, FCT, Lisbon, Text of the 8] discipline of Métodos Computacionais da Engenharia Mecânica. Not edited. 2009/2010.

[1 Filipe Teixeira-Dias, J Alexandre M. Pinho ds Cruz, Robbertt A. F Valente, and Ricardo J 9] de Sousa, *Método dos Elementos Finitos*.: ETEP - Edições Técnicas e Profissionais, 2010.

[2 P. Ferdinand Beer and E. Russel Johnston Jr, *Mecânica Vectorial para Engenheiros*, 6th 0] ed. Alfragide: McGRAW_HILL de Portugal, 1998.

Annex 1 – List of MATLAB mfile

```
% Finite element programme
% The input file, '*.inp', should have:
% - Coordinates of nodes,
% - Definition of elements,
% - Material constants,
% - Sections constants,
% - Loads,
% - Ends,
%
disp('Programa BARRA_3D');
%
% Open of input file
%
tipo={'*.inp'};
titulo='Barra_3D: Seleccione o ficheiro de dados';
[nome,caminho]=uigetfile(tipo,titulo);
ficheiro=[caminho,nome];
disp(nome);
if nome == 0 % Verify if file is found
    warndlg('File not found','Barra_3D');
else
    %
    % Lecture of inputs
    %
    fid= fopen(ficheiro,'r');
    nnos= fscanf(fid,'%d',1);
    fprintf('numero de nos= %3d\n',nnos)
    nos= fscanf(fid,'%f',[3 nnos]);
    nelementos= fscanf(fid,'%d',1);
    fprintf('numero de elementos= %3d\n',nelementos)
    elementos= fscanf(fid,'%f',[4 nelementos]);
    nmateriais= fscanf(fid,'%d',1);
    fprintf('numero de materiais= %3d\n',nmateriais)
    materiais= fscanf(fid,'%f',[1 nmateriais]);
    nseccoes= fscanf(fid,'%d',1);
    fprintf('numero de seccoes= %3d\n',nseccoes);
    seccoes= fscanf(fid,'%f',[1 nseccoes]);
    nforcas= fscanf(fid,'%d',1);
    fprintf('numero de forcas= %3d\n',nforcas)
    forcas= fscanf(fid,'%f',[4 nforcas]);
    napoios= fscanf(fid,'%d',1);
    fprintf('numero de apoios= %3d\n',napoios)
    apoios= fscanf(fid,'%f',[4 napoios]);
    fclose(fid);
    %
    % Change the extension of input file for '*.des'
    %
    dim=size(ficheiro);
```

```
ficheiro(dim(2)-2)='d';
ficheiro(dim(2)-1)='e';
ficheiro(dim(2))='s';
fid= fopen(ficheiro,'w');
fprintf(fid,'Displacements on nodes\n');
%
% Change the extension of input file for '*.esf'
%
dim=size(ficheiro);
ficheiro(dim(2)-2)='e';
ficheiro(dim(2)-1)='s';
ficheiro(dim(2))='f';
fie= fopen(ficheiro,'w');
fprintf(fie,'Forces on elements \n');
%
% Initial calculus
%
ll= zeros(nelementos,1); % Lengths
ff= zeros(nelementos,1); % Axial forces
nos_actuais= nos;        % Nodes position
ug= zeros(3,nnos);       % Displacements
%
for i=1:nelementos
    % Calculate the initial length of elements
    no1= elementos(1,i);
    no2= elementos(2,i);
    dx= nos(1,no2)-nos(1,no1);
    dy= nos(2,no2)-nos(2,no1);
    dz= nos(3,no2)-nos(3,no1);
    ll(i)= sqrt( dx * dx + dy * dy + dz * dz) ;
    % Assigns a value to the initial axial force
    ff(i)= 10;
end
%
% Parameters of control of the Newton-Raphson procedure
% Maximum number of iterations
max= 20000;
% Maximum error
tolerancia= 1e-9;
%
iter= 1;
erro= 9999;
while erro > tolerancia && iter <= max
    % calculs of internal forces
    fprintf('*** iteração %d *** \n',iter);
    %
    f= zeros(nnos*3,1);
    K= zeros(nnos*3);
    %
```

```
% On first iteration the internal forces are not calculate
because they are zero
        %
        if iter > 1
            %fprintf('calculate the internal forces in which
element\n');
            fprintf(fie,' Iter= %d\n',iter);
            %
                fprintf(fie,...
            ' Iter= %d\n  EL ,       FX      ,       FY      ,
FZ     ,   Teta    ,      F    \n',...
            iter);
            for i=1:nelementos
                %
                no1= elementos(1,i);
                no2= elementos(2,i);
                dx= nos_actuais(1,no2)-nos_actuais(1,no1);
                dy= nos_actuais(2,no2)-nos_actuais(2,no1);
                dz= nos_actuais(3,no2)-nos_actuais(3,no1);
                l= sqrt( dx * dx + dy * dy + dz * dz) ;
                mat= elementos(3,i);
                sec= elementos(4,i);
                ae= seccoes(1,sec)*materiais(1,mat);
                ff(i)= ae*(l-ll(i))/ll(i);
                faxial= zeros(2,1);
                ffx(i)=(dx/l)*ff(i);
                ffy(i)=(dy/l)*ff(i);
                ffz(i)=(dz/l)*ff(i);
                teta(i)=(atan(ffy(i)/ffx(i)))*(180/pi);

                faxial(1,1)= -ff(i);
                faxial(2,1)= ff(i);
                %

            fprintf(fie,'   %3d   ,   %12.4e,   %12.4e,   %12.4e,
%12.4e, %12.4e \n',...
                i,ffx(i),ffy(i),ffz(i),teta(i),ff(i));

                % Matrix of transformation
                t= zeros(2,6);
                t(1,1)= dx/l;
                t(1,2)= dy/l;
                t(1,3)= dz/l;
                t(2,4:6)= t(1,1:3);
                %
                fe= t' * faxial;
                % Adds the vector of internal forces to global
forces
                %
                f(no1*3-2:no1*3)= f(no1*3-2:no1*3)-fe(1:3);
                f(no2*3-2:no2*3)= f(no2*3-2:no2*3)-fe(4:6);
```

```
                %
            end % for i=1:nelementos
        end % if iter > 1 ...
        %
        % Assembly of matrix K and the solution of equation
system        %
        for i=1:nelementos
            %
            no1= elementos(1,i);
            no2= elementos(2,i);
            mat= elementos(3,i);
            sec= elementos(4,i);
            dx= nos_actuais(1,no2)-nos_actuais(1,no1);
            dy= nos_actuais(2,no2)-nos_actuais(2,no1);
            dz= nos_actuais(3,no2)-nos_actuais(3,no1);
            l= sqrt( dx * dx + dy * dy + dz * dz) ;
            ae= seccoes(1,sec)*materiais(1,mat);
            l2= l*l;
            ll2= ll(i)*ll(i);
            ll3= ll2*ll(i);
            %
            %   Stiffness   matrix   according   extension   of
Lagrange-Green
            ke= zeros(6);
            ke(1,1)= ae*dx*dx/(ll2*l)+ff(i)*(l2-dx*dx)/ll3;
            ke(2,2)= ae*dy*dy/(ll2*l)+ff(i)*(l2-dy*dy)/ll3;
            ke(3,3)= ae*dz*dz/(ll2*l)+ff(i)*(l2-dz*dz)/ll3;
            ke(1,2)= ae*dx*dy/(ll2*l)-ff(i)*(dx*dy)/ll3;
            ke(1,3)= ae*dx*dz/(ll2*l)-ff(i)*(dx*dz)/ll3;
            ke(2,3)= ae*dy*dz/(ll2*l)-ff(i)*(dy*dz)/ll3;
            ke(2,1)= ke(1,2);
            ke(3,1)= ke(1,3);
            ke(3,2)= ke(2,3);
            %
            ke(1:3,4:6)= -ke(1:3,1:3);
            ke(4:6,1:3)= -ke(1:3,1:3);
            ke(4:6,4:6)= ke(1:3,1:3);
            %
            in=no1*3-2;
            jn=no2*3-2;
            K(in:in+2,in:in+2)=
K(in:in+2,in:in+2)+ke(1:3,1:3);
            K(in:in+2,jn:jn+2)=
K(in:in+2,jn:jn+2)+ke(1:3,4:6);
            K(jn:jn+2,in:in+2)=
K(jn:jn+2,in:in+2)+ke(4:6,1:3);
            K(jn:jn+2,jn:jn+2)=
K(jn:jn+2,jn:jn+2)+ke(4:6,4:6);
            % disp(K);
        end
        %
```

```
        % Calculate the contribution of applied forces to the
global vector of forces
        %
        for i= 1:nforcas
            no= forcas(1,i);
            in=no*3-2;
            f(in:in+2,1)= f(in:in+2,1) + forcas(2:4,i);
        end
        %
        % Penalizes the stiffness matrix due the existence of
ends
        %
        for i= 1:napoios
            no= apoios(1,i);
            in=no*3-2;
            for j=2:4
                if apoios(j,i) == 1
                    K(in+j-2,in+j-2)= K(in+j-2,in+j-2)*1e10;
                end
            end
        end
        %
        % Resolve the equation system
        %
        u= K\f;

        %
        % Print the displacements and refresh several vectors
and matrixes        %
        fprintf(fid,...
            ' Iter= %d\n   No ,       X       ,       Y       ,
Z    \n',...
            iter);
        for i=1:nnos
            %
            % Refresh the global translations             %
            ug(1:3,i)= ug(1:3,i)+u(i*3-2:i*3);
            %
            % Print the displacements
            %
            fprintf(fid,' %3d , %12.4e, %12.4e, %12.4e\n',...
                i,ug(1,i),ug(2,i),ug(3,i));
        end
        %
        % Refresh the nodes coordinates
        %
        nos_actuais= nos + ug;
        for a=1:nnos
        coordenadasx(a)=nos_actuais(1,a);
        coordenadasy(a)=nos_actuais(2,a);
        end
```

```
        % Calculates the error
        %
        erro= u'*u;
        fprintf(fid,'erro= %e\n',erro);
        %
        % Increments the counter of iterations        %
        iter= iter + 1;
        %
    end % while ...

     plot(coordenadasx,coordenadasy,'--rs','LineWidth',2);
            title('Cable trajectory');
            xlabel('x (m)');
            ylabel('y (m)');
end
```

Annex 2 – Input file of programme's A version

11

000

10-7.4190

20-13.0180

30-16.9260

40-19.2350

50-19.9990

60-19.2350

70-16.9260

80-13.0180

90-7.4190

10000

10

1 2 1 1

2 3 1 1

3 4 1 1

4 5 1 1

5 6 1 1

6 7 1 1

7 8 1 1

8 9 1 1

9 10 1 1

10 11 1 1

1

210E9

1

7.069E-4

```
9
2  0 -598.671   0
3  0 -598.671   0
4  0 -598.671   0
5  0 -598.671   0
6  0 -598.671   0
7  0 -598.671   0
8  0 -598.671   0
9  0 -598.671   0
10 0 -598.671   0
2
1  1 1 1
11 1 1 1
```

Annex 3 – "Input" file of programme's B version

```
11
000
10-7.4190
20-13.0180
30-16.9260
40-19.2350
50-19.9990
60-19.2350
70-16.9260
80-13.0180
90-7.4190
1000       0
10
 1  2 1 1
 2  3 1 1
 3  4 1 1
 4  5 1 1
 5  6 1 1
 6  7 1 1
 7  8 1 1
 8  9 1 1
 9   10 1 1
 10  11 1 1
1
210E9
1
7.069E-4
```

```
10
2  0 -598.671   0
3  0 -598.671   0
4  0 -598.671   0
5  0 -598.671   0
6  0 -598.671   0
7  0 -598.671   0
8  0 -598.671   0
9  0 -598.671   0
10 0 -598.671   0
11 3.717e+003 2.694e+003 0
1
1  1 1 1
```

Annex 4 –ANSYS log file

```
!
! Exemplo Catenária
!
/PREP7
N, 1,   0,    0
N, 2,  10,  -7.419
N, 3,  20,  -13.018
N, 4,  30,  -16.926
N, 5,  40,  -19.235
N, 6,  50,  -19.999
N, 7,  60,  -19.235
N, 8,  70,  -16.926
N, 9,  80,  -13.018
N, 10, 90,  -7.419
N, 11, 100,    0
!
! Elemento Barra 2D
!ET,1,LINK1
!R,1,6.4928e-4
!
! Elemento Viga 2D
!ET,1,BEAM3
!KEYOPT,1,6,1
!KEYOPT,1,9,0
!R,1,6.4928e-4,3.349e-8
!
! Elemento Viga 3D (BEAM4)
```

```
!ET,1,BEAM4
!KEYOPT,1,2,1
!KEYOPT,1,6,0
!KEYOPT,1,7,0
!KEYOPT,1,9,0
!R,1,6.4928e-4,3.3537e-8,3.3537e-8
!
! Elemento Viga 3D (BEAM188)
ET,1,BEAM188
SECTYPE,   1, BEAM, CSOLID, cabo, 0
SECOFFSET, CENT
SECDATA,0.015,0,0,0,0,0,0,0,0,0
!
MP,EX,1,210E9          !Módulo de Young
MP,PRXY,1,0.3          !Coeficiente de Poisson
!
E,  1,  2
E,  2,  3
E,  3,  4
E,  4,  5
E,  5,  6
E,  6,  7
E,  7,  8
E,  8,  9
E,  9, 10
E, 10, 11
!
! Forcas concentradas nos Nós
F,2,FY,-598.671
```

```
F,3,FY,-598.671
F,4,FY,-598.671
F,5,FY,-598.671
F,6,FY,-598.671
F,7,FY,-598.671
F,8,FY,-598.671
F,9,FY,-598.671
F,10,FY,-598.671
!
! Densidade e aceleração da Gravidade
!ACEL,0,9.81,0,
!*
!MPTEMP,,,,,,,,
!MPTEMP,1,0
!MPDATA,DENS,1,,7850
!
D,1,UX
D,1,UY
D,1,UZ
D,11,UX
D,11,UY
D,11,UZ
!
FINISH                  !Exits normally from a processor.
!
/SOLU                   !*** SOLUÇÃO ***
SOLCONTROL,0
ANTYPE,STATIC           !Tipo de análise: estática
NEQIT,150
```

```
NLGEOM,ON            !Grandes deslocamentos
SOLVE                !Resolve sistema
/POST1               !*** PÓS-PROCESSAMENTO ***
PRRSOL               !Mostra reacções nos apoios
PRNSOL,DOF           !Mostra deslocamentos e rotações
FINISH               !Exits normally from a processor.
```

Annex 5- Input file of programme for the structural analysis of cable example

16

000

110

240

390

4160

5250

6360

7490

8640

9810

10 100 0

11 121 0

12 144 0

13 169 0

14 196 0

15 225 0

15

1 2 1 1

2 3 1 1

3 4 1 1

4 5 1 1

5 6 1 1

6 7 1 1

7 8 1 1

8 9 1 1

9 10 1 1

10 11 1 1

11 12 1 1

12 13 1 1

13 14 1 1

14 15 1 1

15 16 1 1

1

0.483e9

1

1.539E-4

15

276.0008.8190.000

3142.00018.8900.000

4208.00030.4130.000

5274.00042.1680.000

6340.00053.9990.000

7406.00065.8640.000

8472.00077.7480.000

9538.00089.6440.000

10604.000101.5460.000

11670.000113.4540.000

12736.000125.3650.000

13802.000137.2790.000

14868.000149.1940.000

15934.000161.1110.000

1616000.00027254.6480.000

1

1 1 1 1